4 Radiological Assessment and Its Roles in Head and Neck Surgical Oncology

Luca Bertana, Marco Maria Maceroni, Silvia Karem Janet Flores Quispe, Giacomo Contro, Samuele Frasconi, Matteo Todisco, and Giacomo Spinato

4.1 Introduction of Head and Neck Squamous Cell Carcinoma

Cancers of the head and neck are the sixth most frequent cancer worldwide and are associated with significant morbidity. Head and neck squamous cell carcinoma (HNSCC) represents the most common malignancy, arising from the mucosal epithelium in the oral cavity, pharynx, and larynx [1]. The reported incidence rate in 2008 was 6.8%. From 1990 to 2017, incidence rates for larynx and nasopharyngeal cancers decreased, whereas they increased for other pharyngeal cancers and lip/oral cavity cancers [2]. Geographical variations of incidence rates of HNSCC are related to differences in genetic susceptibility and socio-economic status. In developing countries, such as India and China, exposure to carcinogenic air pollutants and particulate matter is an important risk factor. However, high-risk factors are represented by tobacco consumption (i.e. smoking and betel nut chewing), alcohol, and presence of infectious agents. Persistent infections with human papillomavirus (HPV) and Epstein–Barr virus (EBV) are known aetiological risk factors for HNSCC arising from the oropharynx and nasopharynx, respectively. HPV infection is an increasing risk factor (mainly transmitted by oral sex), particularly for oropharyngeal cancer, most often associated with HPV-16 (secondly HPV-18) [3–6]. In the USA, the cases of HPV-associated oropharyngeal cancers exceed the number of cervix cancers [2].

HNSCC is locally invasive, tends to spread to regional lymph nodes, and has a propensity for perineural spread. A substantial percentage of HNSCC has nodal involvement at initial presentation, and lymphadenopathy may represent the initial complaint. Moreover, lymphadenopathy is an important prognostic indicator in HNSCC, and for this reason, all of the cervical lymph node chains should be evaluated when the primary tumour is imaged [7, 8]. Perineural spread (PNS) is typically retrograde, from the primary site toward the skull base. PNS is a negative prognostic factor, and its presence is an indication for adjuvant radiation therapy [9]. HNSCC can metastasize by hematogenous routes, usually in

L. Bertana (✉) · Silvia Karem Janet Flores Quispe
Radiological Department, General Hospital Ca' Foncello, Treviso, Italy

M. M. Maceroni
Department of Radiological, Oncological and Pathological Sciences, SAPIENZA University of Rome, Sede di Latina I.C.O.T., Latina, Italy

G. Contro · S. Frasconi · G. Spinato
Department of Neurosciences, Section of Otolaryngology and Regional Centre for Head and Neck Cancer, University of Padova, Treviso, Italy

M. Todisco
Unit of Radiology, University Hospital of Padua, Padua, Italy

N. Mat Lazim et al. (eds.), *Head and Neck Surgery : Surgical Landmark and Dissection Guide*,
https://doi.org/10.1007/978-981-19-3854-2_4

advanced disease. The lungs are the most common sites of distant metastases from head and neck cancer followed by bone and liver [10]. Patients with HNSCC have an increased risk of second primary malignancies, predominantly involving the upper aerodigestive tract, but there is also a high incidence of second primary lung cancers. A higher percentage of second primary malignancies are metachronous (i.e. identified at least 6 months after identification of the primary tumour) than synchronous. Following the successful therapy of the primary tumour, second primary tumour has a reported annual incidence of 3–7% [11, 12].

4.1.1 Clinical Presentation and Assessment of Head and Neck Malignancy

HNSCC is a cancer of adults, more frequent in male than in women, with a median age at diagnosis of 66 years for HPV-negative HNSCC, 53 years for HPV-positive HNSCC, and 50 years for EBV-positive HNSCC [6, 13, 14]. The clinical presentation depends on the anatomical site of the primary tumour and tumour extension. Early recognition and diagnosis may improve the survival rate, which depends on the stage of disease and clinical status of the patient. The diagnosis of HNSCC must be established by histologic examination of tissue biopsy [15]. In the setting of oropharyngeal tumour and unknown primary tumour, HPV testing is mandatory as HPV status is a determinant factor in the current staging [6, 16]. Multiple techniques are available for the determination of HPV status, and currently the cheaper and more reliable test is the identification of the upregulation of a cyclin-dependent kinase inhibitor, known as p16 [17].

After the histological diagnosis, the second step to determine the adequate treatment strategy is the tumour staging. In the American Joint Committee on Cancer (AJCC)/Union for International Cancer Control (UICC) cancer staging manuals, staging is described by the primary tumour, nodal disease, and distant (metastatic) spread, designing the TNM system. Oncologists designate a final clinical stage, termed cTNM, after combining information from the physical examination, histological evaluation, radiology findings, sentinel node biopsy, and other diagnostic tests. After tumour resection, the pathological examination enables to provide the pTNM. The cTNM or pTNM may be combined with additional specific factors. In an ideal staging system, each stage group should provide a specific prognosis and accurate outcome prediction, meaning that patients in the same group should have similar survival rates [18].

Currently, both HNSCC stage and HPV status are recognized as the major determinants of HNSCC prognosis. The 8th edition of the Cancer Staging Manual contains three important changes: addition of depth of invasion (DOI) to tumour staging in oral cavity cancers, addition of extracapsular nodal extension (ENE) to nodal staging in non-viral HNSCC, and codification of a novel staging system for HPV-positive HNSCC. Staging of nasopharyngeal carcinoma remains strictly based on anatomy, without incorporation of viral or environmental aetiology. The staging evaluation includes complete head and neck clinical examination and cross-sectional imaging. In fact, clinical examination, with direct inspection and endoscopy as required, permits to visualize the mucosa of the upper aerodigestive tract; however, submucosal and deeper tumours cannot be seen. Cross-sectional imaging allows to establish the extent of locoregional disease, to detect bony invasion and perineural or perivascular spread, to assess lymph node metastases, to rule out distant metastatic disease, and to exclude a second primary tumour [18, 19].

In the treatment planning, there are three points to rule out: evaluating the extension and the boundaries of the tumour, detecting potential infiltration of adjacent structures (e.g. vessels, cranial nerves), and differentiating between tumour infiltration and inflammatory reaction of surrounding tissue. Imaging is not only fundamental in the planning therapy, but also a crucial tool in the follow-up of patients under therapy, to evaluate response to treatment, and to detect recurrences before it becomes clinically evident. Treatment is generally multimodal, consisting of

surgery resection, radiotherapy, and chemotherapy. Pathological features indicative of increased risk of recurrence include extranodal extension, close or involved surgical margins, or perineural invasion [20].

4.1.2 Cross-Sectional Imaging of Head and Neck Tumours

Imaging modalities available include computed tomography (CT), magnetic resonance imaging (MRI), ultrasound (US), and positron emission tomography/computed tomography (PET/CT). When staging HNSCC, the tumour sites, availability of the imaging modality, patient compliance to the imaging evaluation, and possible contraindications should be considered. Imaging examinations should be performed with intravenous contrast medium, and its related contraindications must be taken into account. A well-known contraindication of MRI is the presence of ferromagnetic devices, due to the magnetic field that can displace implants, affect the function of devices, and cause tissue heating [11].

CT is usually the first imaging modality used for the staging process, thanks to its wide availability, reproducibility, and high space resolution. CT can provide information on primary tumour extent, cervical lymph node metastasis, and bone involvement with short scan times. However, low soft-tissue resolution will not always enable the visualization of exact lesion boundaries, particularly in the context of surrounding soft tissues with similar attenuation. Visualization of vestibule mucosa can be improved using the 'puffed-cheek manoeuvre', resulting in dilatation of the vestibule with air and separation of the mucosal surfaces [11, 21].

However, CT can have limitations in the oral region, due to the metal artefacts from dental amalgams and beam hardening from adjacent mandible and maxilla. However, many advances have contributed to reducing metal artefacts. New software algorithms including iterative metal artefact reduction (IMAR) have contributed to improved metal artefact reduction. Dual-energy CT with various supplementary reconstructions may gain a relevant role in the imaging evaluation, thanks to various supplementary reconstructions for artefact reduction and improvement of soft-tissue contrast [20, 22].

MRI offers a superior soft-tissue contrast compared to CT, providing a better delineation of soft-tissue invasion. MRI is the preferred staging tool for nasopharyngeal carcinoma, enabling the detection of skull base infiltration (T3) or intracranial extension of disease (T4) [23, 24]. MRI is often used for the study of oral cavity and oropharynx, due to the high soft-tissue contrast enabling the detection of small primary tonsillar tumours and evaluating the deep extent of an infiltrative lesion when planning surgical resection or intensity-modulated radiation therapy [21]. In the larynx, CT is the preferred imaging modality, due to MRI motion artefact in this anatomic district. MRI may be reserved for cases of uncertain cartilage invasion (T4a) [25]. Nodal disease can be evaluated with CT, MR, and US, as described subsequently.

In PET/CT examination, it is important to know that different tissues have variable degrees of normal FDG uptake, particularly muscles, brown fat, salivary and lymphoid tissue, and recent biopsy sites. These all serve as potential false-positive pitfalls in PET imaging. A potential false-negative finding is the absence of uptake in a predominantly cystic node. Correlation with neck CT imaging will allow correct identification of cystic nodal metastases. US has a limited role in HNSCC, mainly reserved for interrogation of nodes that are equivocal on other imaging modalities, and particularly when a positive finding, such as a contralateral node, might significantly alter staging and management. US can also serve as an imaging guidance for fine needle aspiration [7].

4.2 Preoperative Imaging Evaluation

Cross-sectional imaging has a fundamental role in the preoperative tumour evaluation. Together with clinical and histological examination, imaging provides information required for the tumour staging. In the treatment planning, preoperative

imaging is fundamental to evaluate particular spread or tumour extension: perineural tumour spread, carotid involvement, invasion of prevertebral space, and bone or cartilage invasion. Lymph node evaluation is discussed separately.

4.2.1 Perineural Tumour Spread

In head and neck tumours, perineural spread (PNS) represents an important route of spread, extending along the nerves. PNS is common in adenoid cystic carcinoma, HNSCC, and salivary duct carcinoma. Currently, PNS is considered an independent prognostic indicator, associated with a nearly threefold increase in local recurrence and approximately 30% decrease in 5-year survival rate. In almost 50% of patients, PNS can be asymptomatic. The most commonly involved nerves are the trigeminal and facial nerves. Typically, perineural spread is retrograde toward the skull base; however, antegrade spread can also occur from branch points. The high soft-tissue contrast resolution makes MRI the optimal imaging modality for the detection of direct signs of PNS along a nerve: contrast enhancement and enlargement (Fig. 4.1). Nerve enlargement can lead to obliteration of the perineural fat tissue at foraminal openings or fissures. Further involvement can result in bone changes, such as foramina/fissure widening and bone erosion, better evaluated on CT. Muscle denervation changes are indirect signs of PNS. In the acute or subacute phase of denervation, muscle oedema and increased enhancement are typical findings. Chronic denervation results in fatty replacement and muscle atrophy. Differential diagnoses of PNS in case of nerve enlargement or enhancement are primary nerve tumours and inflammatory and infectious conditions. In case of bone changes, differential diagnoses are radionecrosis and odontogenic infections [26, 27].

4.2.2 Carotid Artery Involvement

Carotid space, often referred to as the retrostyloid compartment of the parapharyngeal space, is an important landmark in treatment planning. Besides the carotid arteries (i.e. common carotid and internal carotid arteries, and a portion of the external carotid artery and the internal jugular vein), the nerve structures contained in the carotid space should be kept in mind: cranial nerves IX, X, XI, and XII; cervical sympathetic trunk; and ansa cervicalis, a part of the cervical plexus. Preoperative

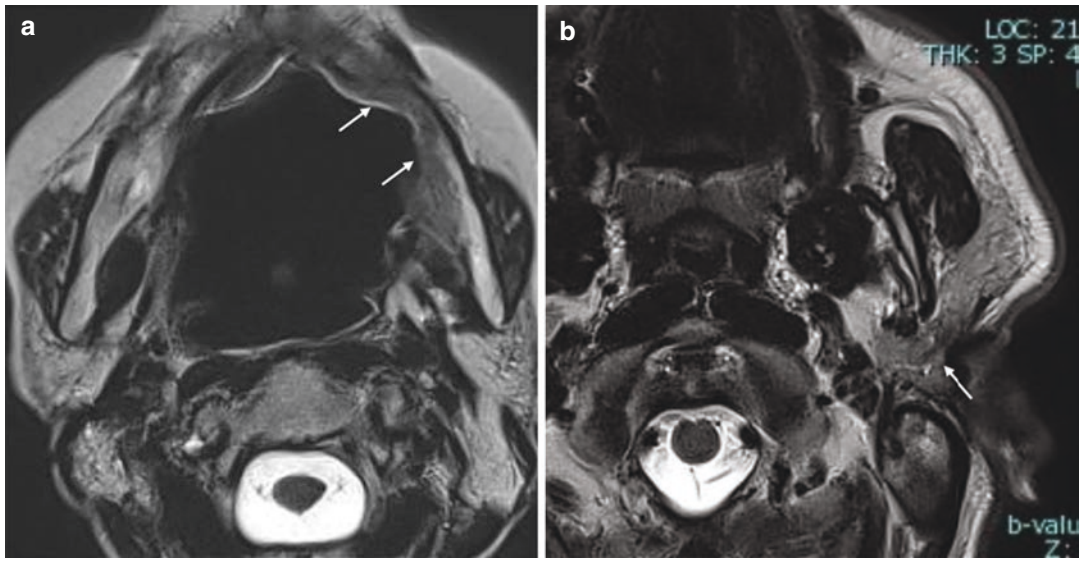

Fig. 4.1 Perineural spread. (**a**) Enlargement of inferior alveolar nerve and its canal (white arrow). (**b**) Auriculotemporal nerve enlargement from squamous cell carcinoma of the skin (white arrow)

evaluation of direct invasion of carotid space has staging and treatment implications, identifying patients with poor prognosis. Moreover, also a metastatic lymph node can invade the carotid artery. According to the 8th AJCC, in case of oropharyngeal non-HPV-associated squamous cell carcinoma, encasement of the carotid artery upstages the lesion to T4b disease. Hence, involvement of carotid sheath is a critical issue in tumour resectability, and there are three possible settings: unresectable tumour, resectable tumour with limited 'collateral damage' and morbidity, and resectable tumour requiring extensive complicated surgery with related quality-of-life issues.

Radiological criteria of carotid involvement in literature are carotid encasement defined as more than 270° of circumferential contact of the tumour with the vessel (Fig. 4.2), obliteration of the fat between the lymph node/primary tumour and the carotid artery, deformation of the carotid artery, and length of contact between the carotid artery and tumour mass. Several studies have been conducted to classify carotid invasion on preoperative imaging including US, MRI, and CT. Currently, MRI can be considered the most sensitive imaging modality to detect carotid encasement [28, 29].

4.2.3 Invasion of Prevertebral Space

Prevertebral space involvement is associated with poor outcomes, due to the high rate of adenopathy (in particular retropharyngeal nodes) and local recurrence, and even hematogenous metastases are increased. Tumour fixation to the longus colli/capitis muscle complex implies an incomplete surgical resection; hence, detection of this extension is fundamental to define tumour resectability. MRI provides higher soft-tissue contrast and more anatomic detail than CT, visualizing the preservation of the retropharyngeal fat planes [30, 31].

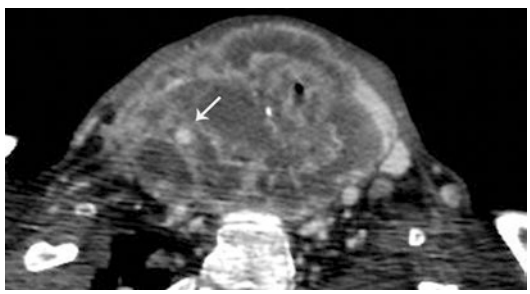

Fig. 4.2 Carotid artery encasement by the tumour

4.2.4 Bone and Cartilage Invasion

Bone and cartilage invasion is a decision-making information in the planning treatment, in particular for oral and laryngeal cancer, respectively. In the setting of oral cancer, preoperative evaluation of mandibular invasion is critical for planning the type of mandibular resection. The common route of spread is along the buccal cortices, where a wide bone invasion may be detectable even in a clinical examination. However, imaging is the appropriate tool to detect bone invasion, specifying the extension of involvement. Bone involvement can vary from superficial cortical to deep cortical to marrow invasion and mandibular canal involvement. CT is generally considered superior for detection of bone invasion, in particular for early cortical erosion. However, MRI permits the identification of marrow invasion and has a high negative predictive value, demonstrating also marrow replacement without grossly visible cortical breakthrough. Hence, CT and MRI result to be complementary imaging modalities for the evaluation of bone invasion (Fig. 4.3) [32, 33].

Also, in the setting of laryngeal cancer, CT has a primary role in the detection of cartilage invasion. Classical criteria of tumour invasion of the thyroid cartilage are erosion, lysis, and transmural extralaryngeal tumour spread. Extralaryngeal spread can be considered in case of substitution by tumour tissue on the outside of the membrane/cartilage, or obliteration of fat tissue between the extralaryngeal structure and laryngeal components. In case of subtle cartilage invasion, CT alone may result to be insufficient, and MRI can be useful for excluding cartilage invasion. Moreover, there is an increasing role of dual-energy CT [25, 34].

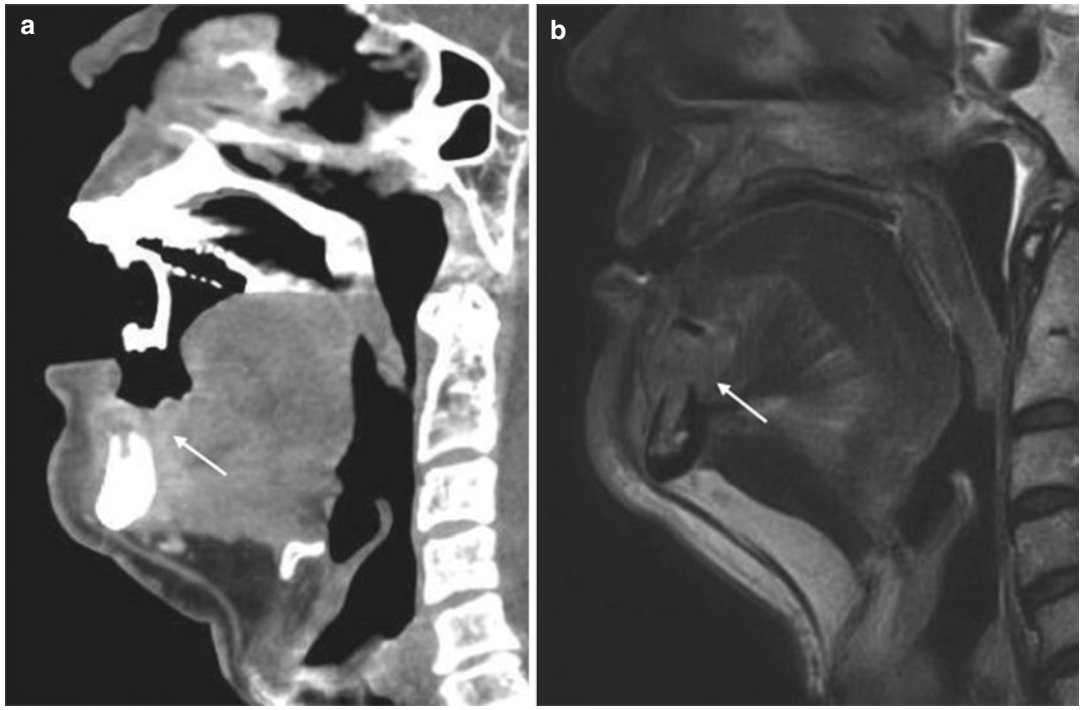

Fig. 4.3 Mandibular bone invasion (white arrow) from squamous cell carcinoma of the head and neck. (**a**) CT scan. (**b**) MR T2w image

4.3 Imaging Highlights of Head and Neck Anatomy

Head and neck anatomy is complex, and on cross-sectional imaging, various anatomical spaces are defined by the presence of fascial planes. However, the main anatomic subdivision concerns the aerodigestive tract, defining the oral cavity, the three regions of pharynx (i.e. nasopharynx, oropharynx, and hypopharynx), and the larynx. The definition of these portions is useful from a clinical point of view because malignancies such as HNSCC tend to differ in presentation, routes of spread, and clinical management.

4.3.1 Oral Cavity

The oral cavity is the most ventral portion of the aerodigestive tract and is separated from the oropharynx by the circumvallate papillae, the anterior tonsillar pillars, and a line connecting the upper margins of the tonsillar pillars along the soft palate. The oral cavity includes the oral tongue (anterior two-thirds of the tongue), floor of the mouth (FOM), lips (inner mucosal surface of the lips), gingivobuccal and buccomasseteric regions, and adjacent portions of the maxilla and mandible. The tongue consists of two symmetric halves, divided by a midline septum, and it is composed of muscular tissue distinguished in intrinsic and extrinsic muscles. The extrinsic muscles provide attachment of the tongue to the hyoid bone, mandible, and styloid process, and they are represented by genioglossus, hyoglossus, styloglossus muscles, and palatoglossus. The FOM is a U-shaped structure where the mylohyoid muscles represent the primary supporting structure. Additional support structures are represented by the paired paramedian geniohyoid muscles and the anterior bellies of digastric muscles.

The retromolar trigone (RMT) is an important landmark of tumour spread. It is defined as a triangular area of mucosa posterior to the lower and upper third molars covering the anterior surface of the lower ascending ramus of the mandible. It is located at the crossroads of buccal, masticator,

and parapharyngeal spaces. Squamous cell carcinomas at this site are frequently diagnosed at an advanced stage, are prone to bone invasion, and tend to have a poor prognosis.

The pterygomandibular raphe, a thick fascial band between the hamulus of the medial pterygoid plate, and the posterior border of the mylohyoid ridge of the mandible may represent the route of spread of RMT lesions. The pterygomandibular raphe is also defined as the line of attachment for the buccinator and superior pharyngeal constrictor muscles at the junction of the oropharynx and oral cavity. The glossomylohyoid gap is another pathway of spread. It is identified between the mylohyoid and the lateral glossal muscle group (i.e. hyoglossus, styloglossus, and palatoglossus muscles) and provides a communication between the sublingual and submandibular spaces [21, 32].

4.3.2 Nasopharynx

The nasopharynx is the cranial section of the pharynx, extending from the skull base to the level of the hard palate. The lateral walls are formed and supported by the margins of the superior constrictor muscle and the pharyngobasilar fascia. The nasopharynx is in communication with the middle ear via the Eustachian tube. Next to the opening structure of the Eustachian tube (torus tubarius), there is the fossa of Rosenmüller, a common site of origin of nasopharyngeal cancer. The pathway of access for the Eustachian tube and levator veli palatini muscle through the pharyngobasilar fascia is represented by the sinus of Morgagni.

The anatomy of the central skull base is a fundamental knowledge to understand the pathways of perineural spread. It should be reminded that in the region of Meckel's cave, the trigeminal nerve (V) forms three branches: the ophthalmic nerve (V1) extends through the superior orbital fissure; the maxillary nerve (V2) extends through the foramen rotundum into the pterygopalatine fossa where it branches into the infraorbital nerve and palatine nerves; and the mandibular nerve (V3) exits through the foramen ovale. An important landmark is represented by the pterygopalatine fossa, containing fat, branches of the maxillary nerve, pterygopalatine ganglion, and small vessels. The foramen rotundum and the vidian canal enter the pterygopalatine fossa [24].

Sinus of Morgagni may represent the route of spread for cancer to the parapharyngeal space and skull base. Perineural spread along the mandibular nerve (V3) can cause an intracranial extension. Further intracranial spread may involve the cavernous sinus, Meckel's cave, and prepontine cistern. Anterior tumour extension may involve sinonasal cavities and pterygopalatine fossa, allowing perineural spread. Tumour extension into the carotid space may permit perineural spread in cranial nerves IX to XI. The retropharyngeal nodes are the primary nodal drainage in nasopharynx [35].

4.3.3 Oropharynx

The oropharynx is posterior to the oral cavity and includes the tongue base, palatine tonsils, posterior tonsillar pillars, soft palate, and constrictor muscles. Bilaterally, the tonsillar fossa, containing the palatine tonsil, is delimited by the anterior tonsillar pillar made up by the palatoglossus muscle, and the posterior pillar formed by the palatopharyngeus muscle. The mucosa and the musculature are surrounded by the visceral fascia. Posterior tumour extension can cause disruption of the visceral fascia and invasion of longus capitis and colli muscles and the vertebrae. Lateral tumour extension may invade the parapharyngeal space and the carotid space [32].

4.3.4 Hypopharynx

The hypopharynx or laryngopharynx, which extends from the level of the hyoid bone to the upper margin of the cricopharyngeus muscle, is at the lower level of the cricoid cartilage. The post-cricoid region is the anterior wall of the hypopharynx. The posterior wall of the hypopharynx represents the continuation of the posterior wall of the oropharynx. The lateral recesses of the hypopharynx are defined by the pyriform sinuses, which in most caudal portions are located

at the level of the true vocal cords. The medial wall of the pyriform sinus is formed by the lateral surface of the aryepiglottic fold. Squamous cell carcinoma of hypopharynx commonly arises in the pyriform sinus [25, 36].

4.3.5 Larynx

The larynx can be distinguished in three portions: supraglottic larynx, glottis, and subglottic larynx. The supraglottic larynx extends from the tip of the epiglottis to the level of the laryngeal ventricle. The glottis includes the anterior and posterior commissure at the level of the true vocal folds. The subglottic larynx extends below the glottis to the level of the lower margin of the cricoid cartilage. The hyaline cartilaginous structures included in the larynx are the thyroid cartilage, cricoid cartilage, arytenoid cartilage, and corniculate cartilage. The cricoid, thyroid, and arytenoid cartilages are all hyaline cartilages, and there are various degrees of ossification. Cartilage evaluation may be difficult due to the common asymmetric ossification. Ossified areas tend to be more sensitive to cancer invasion in comparison with cartilaginous areas. The epiglottis consists of yellow elastic fibrocartilage and seldom calcifies. The epiglottis has a laryngeal surface and a lingual surface, with a superior portion extending above the level of the hyoid bone although considered supraglottic. The larynx is delimited anteriorly by thyrohyoid membrane. A common route of tumour spread from the larynx is through areas of weakness via the thyrohyoid membrane (Fig. 4.4). Another route of extralaryngeal spread

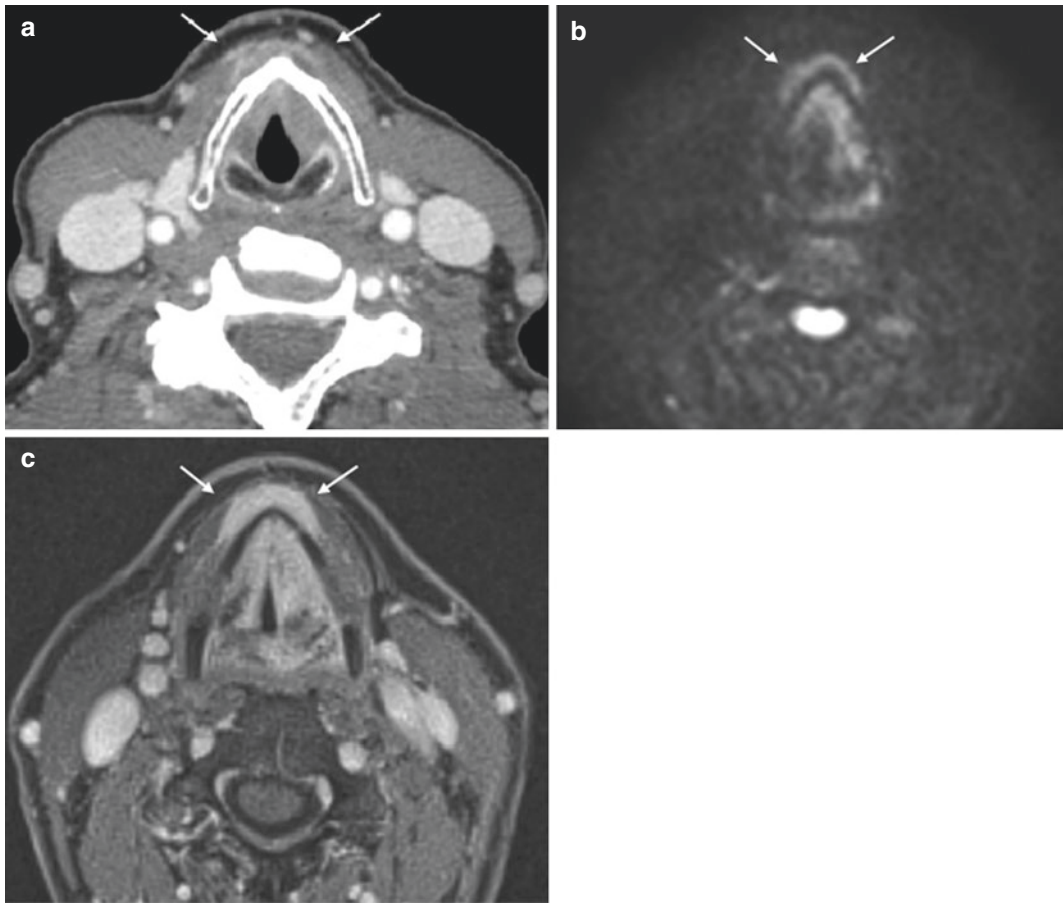

Fig. 4.4 Laryngeal cancer T4: invasion of tissue beyond the larynx with involvement of strap muscles (white arrows). (**a**) CT scan. (**b**) High-resolution DWI. (**c**) 3D T1w post-contrast

is via the inferior pharyngeal constrictor muscle. Submucosal extension may permit the extralaryngeal extension via the cricothyroid membrane [25, 34].

4.4 The AJCC Head and Neck Tumour Classification Changes

The 8th edition of the AJCC has introduced changes that reflect new advances in the knowledge of pathophysiology of these cancers. Moreover, in response to growing evidence of prognostic relevance, additional criteria have been added: the depth of invasion and extranodal extension [7, 18, 23]. Subsequently, the major changes are summarized.

4.4.1 Oral Cavity Squamous Cell Carcinoma

In the 8th edition of the AJCC staging system, tumours arising from the external dry lip are considered cutaneous carcinomas. Tumours arising from the inner lip, which is a wet mucosal surface, are still considered to be oral cavity tumours. Oral cancers are typically asymptomatic and painless at an early stage; thus, intraoral lesions can be diagnosed at advanced stage. The most commonly affected sites are the floor of the mouth and the lateral and ventral aspects of the tongue with less frequent involvement of the retromolar trigone (RMT), buccal mucosa, maxillary and mandibular gingiva, and mucosal lining of the hard palate. Intraoral lesions tend to be diagnosed at a more advanced stage. Oral cavity tumour staging has undergone a substantial alteration, with removal of the criterion of extrinsic muscle invasion for T4 category, which is most relevant for oral tongue malignancies. This is a criterion that was frequently determined by radiologic evaluation since pathologists often have difficulty distinguishing extrinsic from intrinsic muscle invasion. The depth of invasion (DOI) is a new pathologic criterion for determining T status, according to the recognition of its prognostic significance. This pathologic measurement, at surgical resection, is different from the total thickness of the tumour (Fig. 4.5). The accuracy of CT and MRI for determining the depth of invasion and therefore permitting more accurate preoperative tumour staging for oral cavity lesions remains to be proven.

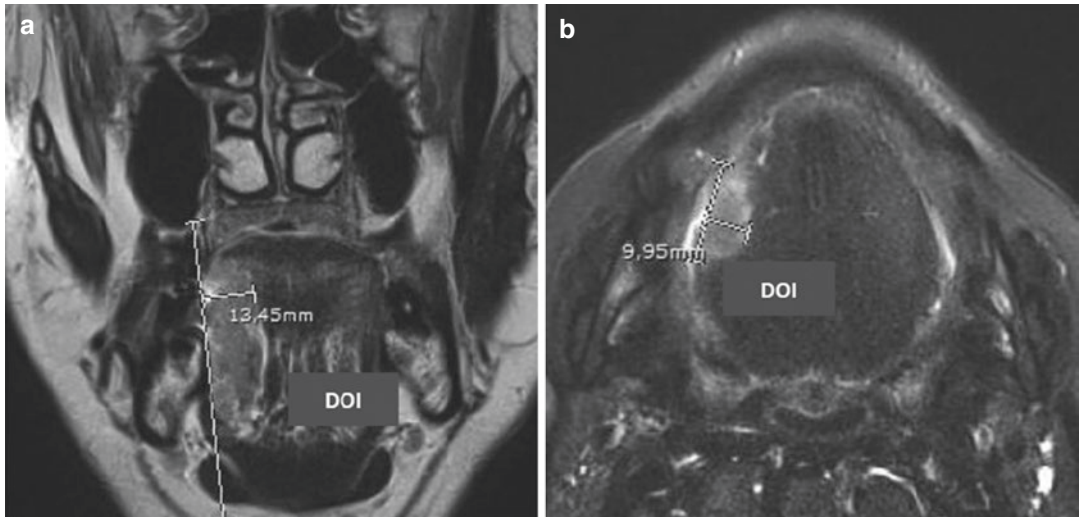

Fig. 4.5 Tongue cancer. (**a**) T3 lesion with DOI of 13 mm. (**b**) T2 lesion with DOI of 10 mm

4.4.2 Oropharyngeal Squamous Cell Carcinoma

It has been stated that an oropharyngeal squamous cell carcinoma (OPSCC) that demonstrates the positivity HPV status (i.e. p16 positive at immunohistochemistry test) shows a better prognosis than p16 negative, which is often associated with tobacco and alcohol (Fig. 4.5). The AJCC7 designated stage III disease when one metastatic OPSCC node is identified and stage IV disease for more than one node or a node larger than 3 cm. HPV-mediated OPSCC has a tendency to present with multiple or large nodes, and such cases, with the prior staging system, were frequently designated as stage IV despite an overall survival rate of around 90%. The AJCC8 proposed a new staging system for HPV-associated OPSCC, stating that all ipsilateral nodal diseases are to be designated as N1, bilateral or contralateral nodes are to be designated as N2, and nodes that are larger than 6 cm are to be designated as N3. Stage I is determined by T1–2 and N0–1, stage II by T1–2 and N2 or T3 and N0–2, and stage III by T4 or N3. Stage IV is reserved for patients with metastatic disease. Thus, patients with a small primary tumour and multiple ipsilateral nodes would now be staged as T1N1, stage I. With AJCC8 staging, up to 80% of patients with HPV-associated OPSCC will be stage I with a 90% 5-year overall survival. A small percentage of patents will have metastatic disease and be stage IV with a 20% 5-year overall survival rate. In case of tumour resection, nodal evaluation in the pTNM system diverges from the clinical nodal system, with N1 being defined by the presence of four or fewer positive nodes and N2 being defined as the presence of more than four malignant nodes, removing the N3. However, at many institutions, OPSCC remains to be treated with definitive chemoradiation therapy, which obviates this somewhat confusing pathologic nodal category. Hence, for radiologists, the HPV status of OPSCC is a fundamental information.

The only modification to the T category that occurs in HPV-associated OPSCC is that T4 is not separated into two categories (Fig. 4.6). T4 is described as tumour invading the larynx, extrinsic muscles of the tongue, medial pterygoid, hard palate or mandible, or beyond.

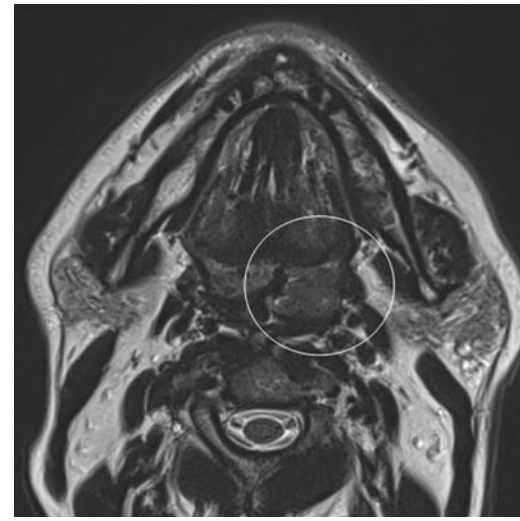

Fig. 4.6 Carcinoma of the tonsil, oropharynx, p16+, T3 lesion with max diameter of 43 mm. T2w image

4.4.3 Nasopharyngeal Squamous Cell Carcinoma

In nasopharyngeal cancer, clinical presentation depends on tumour size and extent as well as cervical nodal metastasis. Metastatic adenopathy is often the initial complaint, and it is independent of tumour size. A serous otitis media can occur due to Eustachian tube obstruction. Advanced lesions may present with neurologic signs secondary to perineural spread or invasion of the skull base. Involvement of the cavernous sinus may produce neuropathies of cranial nerves III, IV, V, or VI. Posterior spread to the carotid sheath may lead to the involvement of cranial nerves IX, X, or XI or sympathetic chain.

Even if NPC is often related to EBV, currently there is not a separate staging system for non-EBV- and EBV-associated NPC. According to the prognosis, the involvement of the pterygoid muscles, previously categorized as T4, has now been reduced to T2. The infiltration is categorized as T4 when a tumour is more extended, in particular lateral to the lateral pterygoid and into the parotid gland. The terms masticator space and

infratemporal fossa, which were part of the AJCC7 terminology, have been removed and replaced with specifically named soft-tissue structures to simplify and clarify staging. In AJCC8, the nodes in levels IV and VB are designated N3 disease. Also, nodal masses larger than 6 cm are in N3 category with removal of the prior subgroups. In AJCC8, N3 now determines a prognostic stage grouping of IVA, rather than IVB.

4.4.4 Non-HPV Oropharyngeal Squamous Cell Carcinoma

The 8th edition of AJCC has introduced a modification in N designation in case of metastatic nodes of non-HPV oropharyngeal cancers, and no changes in T designation. Whereas the criteria of N1–N3 are foundationally unchanged, in comparison to AJCC7, an additional clinical criterion of extranodal extension (ENE) has been added, which determines N3b status. New pathologic nodal table also incorporates pathologic ENE. Pathologic ENE is described as 2 mm or less for microscopic ENE or more than 2 mm for major ENE. In literature, the radiological definition includes different features, such as indistinct nodal margins, irregular nodal capsular enhancement, interruption in the nodal capsule, or infiltration into the perinodal fat or into adjacent muscle.

4.4.5 Unknown Primary Tumours

An unknown primary tumour is defined as HNSCC detected from fine needle aspiration of a nodal mass in the absence of a clinically evident primary source. Most of these cases are from HPV-related tumour. In adult patients, a new neck mass must be first of all suspicious for carcinoma (commonly primary oropharyngeal tumour), and a FNA should be performed. If p16 is positive and no oropharyngeal primary is clearly found at cross-sectional imaging or tonsillectomy, then HPV in situ hybridization is recommended because p16 can be positive in non-HPV-related, non-oropharyngeal tumours, including up to 30% of skin cancers.

4.4.6 Tumour Types Without Changes from the 7th Edition of AJCC

For all non-HPV, there are no changes to the T designation. There are no changes to the T designation also for salivary neoplasms, and to nasal cavity and paranasal sinus tumours. Criteria for T4b cancers remain, i.e. the vascular encasement and invasion, prevertebral space invasion, and invasion of mediastinal structures.

4.5 Lymph Nodes

4.5.1 Introduction

The assessment of lymph node metastasis in head and neck oncology is a critical prognostic factor in terms of treatment planning and patient survival. Metastasis can arise from primary head and neck squamous cell carcinoma (HNSCC), thyroid gland, skin, or distant sites like melanoma, or breast, lung, or gastrointestinal carcinomas. The presence of cervical nodal metastasis may affect the choice of treatment as well as the patient prognosis. With a single lymph node metastasis from HNSCC of the head and neck, a patient's 5-year survival rate is estimated at 50%, which is reduced to 33% in the presence of contralateral lymph node involvement. More than 50% of advanced stages of HNSCC as T3–T4 show ipsilateral nodal metastasis, whereas 2–35% have bilateral or contralateral nodal metastasis [37]. For these reasons, detecting cervical lymph node metastasis is an essential step in predicting patient prognosis and evaluating treatment options. Treatment options in cases of cervical lymph node metastasis include selective, radical, or modified neck dissection and co-adjuvant radiotherapy and/or chemotherapy depending on the histologic findings of the nodes.

Imaging has a central role in the diagnosis and follow-up of cervical lymphadenopathies. The

American Joint Committee on Cancer has stated that clinical staging should include physical examination as well as results of the imaging modalities. The National Comprehensive Cancer Network (NCCN) guidelines recommend the use of CT and MR with contrast medium for the initial staging in patients with HNSCC [38]. However, clinical criteria alone are not sufficiently accurate in the identification of nodal metastasis. The detection rate of nodal involvement with palpation has an accuracy rate of 70% [39, 40]. Furthermore, deep-seated nodes such as the retropharyngeal type can be properly evaluated exclusively with the support of imaging modalities.

Radiologic evaluation of head-neck nodes has shown to identify metastasis in 7–19% of patients with a negative clinical evaluation. In case of positive imaging results, even in the presence of low pretest likelihood for potential nodal metastasis, the risk of positive nodal metastasis remains very high (estimated at >20%) [41] and so elective neck dissection should be performed in all cases when positive radiologic findings for potential nodal metastasis are present. Different imaging modalities exist for identifying cervical nodal metastasis, including ultrasound (US), computer tomography (CT), magnetic resonance (MR), and CT/positron emission tomography (PET).

Currently, the use of preoperative MR or CT imaging is an essential part of the workup. Both modalities have demonstrated good diagnostic performance in detecting head-neck nodal metastasis, even if no significant diagnostic accuracy had been found in comparison with the other modalities. CT and MR should be preferred to the other imaging modalities in the assessment of primary radiologic staging, as it has the advantage of being able to evaluate both primary tumour 'T' and nodal involvement 'N' [42, 43] and for nodal surveillance especially in patients with an advanced tumour, when the site of the primary tumour also requires surveillance of the deep-seated lymph node as in the case of the nasopharyngeal SCC and when neck dissection is performed. PET is an expensive exam, is generally less available, and does not provide any better sensitivity and specificity in the detection of nodal metastasis. It therefore should not be used in routine nodal surveillance.

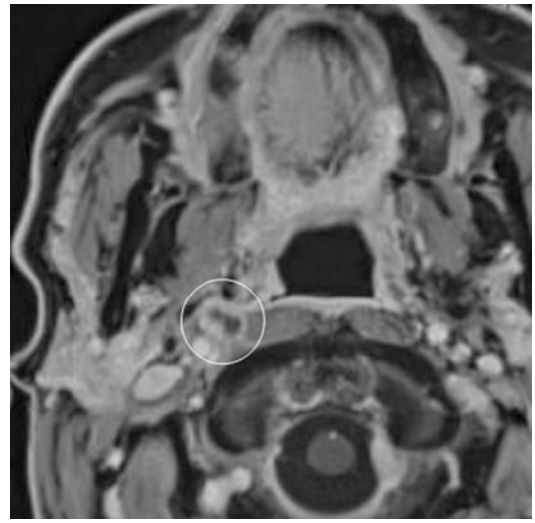

Fig. 4.7 Right single Rouviere nodal metastasis with central necrosis from oropharynx carcinoma

The lack of ionizing radiation and the relative low cost of US mean that this method can be used more frequently than CT and MR. US demonstrates similar sensitivity and specificity to other modalities and can be used with concomitant real-time-guided fine needle aspiration (US-FNA); however, deep-seated lymph nodes cannot be identified with this method (Fig. 4.7). US should be considered as the modality of choice in the follow-up of the cervical lymph nodes in patients with a low-grade HNSCC, such as T1–2 N0 of the lips, when a 'watchful waiting' policy is adopted. Furthermore, in the case of positive or inconclusive US findings, US-FNA should be used due to the high correlation between positive cytology results and histologic positive findings for nodal metastasis [41].

4.5.2 Radiologic Criteria for Assessment of Head-Neck Lymph Nodes

The radiological evaluation of the neck lymph nodes is based on the criteria that identify abnormal lymph nodes in imaging: characteristics that increase the level of suspicion of the presence of

intranodal metastases and that help the radiologist to discriminate these lymph nodes from hyperplastic ones. It is based on five main features: clustering, morphology, inhomogeneity, size, and pattern of spread.

4.5.2.1 Clustering

Clustered lymphadenopathy is recognized as groups of >3 contiguous enlarged lymph nodes with the loss of fat tissue planes between them. This clustering appearance, particularly evident in HNSCC, is associated with a poorer prognosis than isolated lymph node metastasis. This feature can increase the level of suspicion when the size of nodes is borderline [44]. In the presence of reactive adenopathy secondary to infectious process, surgery, or radiation, the detection accuracy is reduced for clustering.

4.5.2.2 Morphology

A normal lymph node appearance is a reniform shape with smooth well-defined margins. Abnormal lymph nodes are defined on imaging as nodes with altered shape and margins. A reniform or oblong shape is more representative of normal nodes, whereas lymph nodes with spherical appearance suggest the presence of an expansive process and are more associated with metastases (Fig. 4.8).

To classify a round lymph node on imaging, the criterion of a long-to-short axis is used, and a ratio of less than 2 is more correlated with metastases. To correctly calculate the long-to-short axis with CT and MR, it is not correct to measure the lymph nodes only on the axial plane. This is because it would not identify the real major axis of the lymph nodes that in the neck-head area is almost always oriented on a cranio-caudal direction. It is therefore recommended that multiplanar reconstructions (MPR) be used in order to correctly identify the major and minor axis. Benign hyperplastic adenopathies, even if they are enlarged in terms of the size criteria, usually maintain a long-to-short axis greater than 2. Shape is important but is not the only aspect to include in the evaluation of suspicious nodes. Roundness alone does not necessarily imply the presence of intranodal metastasis and must be considered with respect to all other worrisome features, above all if the lymph node level involved can be traced back to primary neoplasia (sentinel node). This criterion can be helpful in increasing the level of suspicion in case of enlarged lymph nodes, such as in SCC of the tongue where it is not uncommon to find intranodal metastases in sub-centimetric lymph node at level III. Intranodal metastasis proliferation can replace normal fatty hila; however, this can also be present in infectious processes and in chronic inflammatory lymphadenopathies. In addition, fatty hila may be so thin that it is indistinguishable at CT and MRI (if less than 3 mm) from an

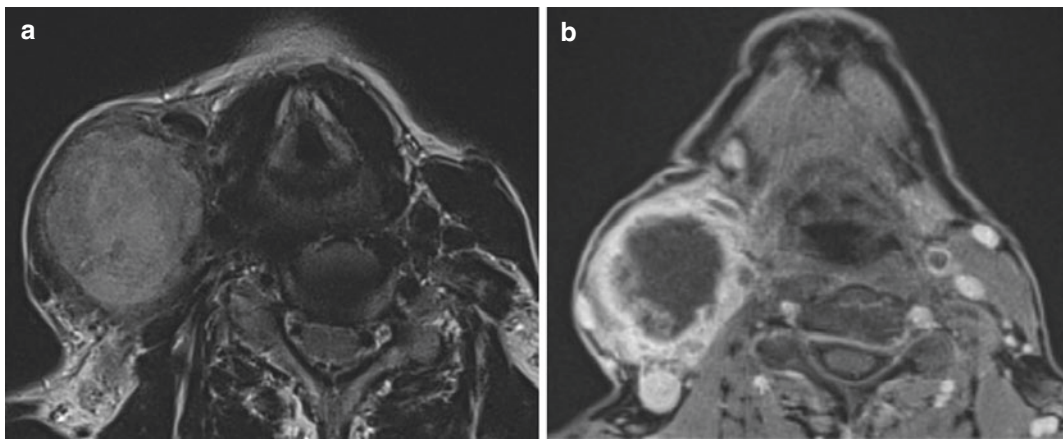

Fig. 4.8 Multiple lymphadenopathies (**a**, **b**) with round morphology and intranodal inhomogeneity, due to necrosis and extranodal extension (ENE+)

initial central necrosis area. In cases where there is doubt, US can be used as a second tool in conjunction with cytology.

In the pathological lymph node, the subcapsular proliferation of metastatic foci causes an alteration of the node margins that can change from smooth and regular to thick, irregular, blurred, or indistinct. The CT is more accurate than other methods for the evaluation of extranodal diffusion; however, both CT and MR are valid methods for this evaluation. Irregular or ill-defined margins on CT and MR are features that significantly improve the detection of cervical lymph node metastases. The extranodal extension (ENE) represents the most important prognostic factor in terms of survival, operability, and comorbidity, with the exception of tumours associated with HPV infection. Only unquestionable clinical evidence is to be used for clinical staging.

The guiding principle is to assign ENE negative if there are doubts in a particular case in order to avoid stage migration, with the concept that whenever there is a doubt, the lesser stage should be chosen. Only clear evidence of gross ENE on clinical examination supported by strong radiographic evidence permits classification of disease as ENEc [45]. Extracapsular spread is microscopically present in 25% of nodes that do not meet the size criteria for suspicion, enlarged lymph nodes smaller than 3 cm are demonstrated to have an incidence of 60% extracapsular spread, whereas nodes larger than 3 cm have an incidence of 74% [37]. Imaging findings of extracapsular spread are indistinct or blurred margins, fat stranding, and loss of fat planes between the lymph node and the surrounding anatomical structure. Pathological lymph nodes can infiltrate adjacent structures such as vessels, nerves, muscles, skin, and bone. CT and MR have been shown to have low sensitivity (65–80%) but high specificity (86–93%) for the detection of ENE (Fig. 4.9) [45]. Arterial invasion influences the surgical options and can lead to dangerous complications (pseudoaneurysms, vascular occlusions). Identification of arterial encasement >di 270° on CT or MR is associated with increased likelihood of arterial invasion with a sensitivity and specificity [46].

4.5.2.3 Inhomogeneity

Metastatic lymph nodes have a heterogeneous structure represented by a portion of the healthy lymph node and part of the tumour process. Very

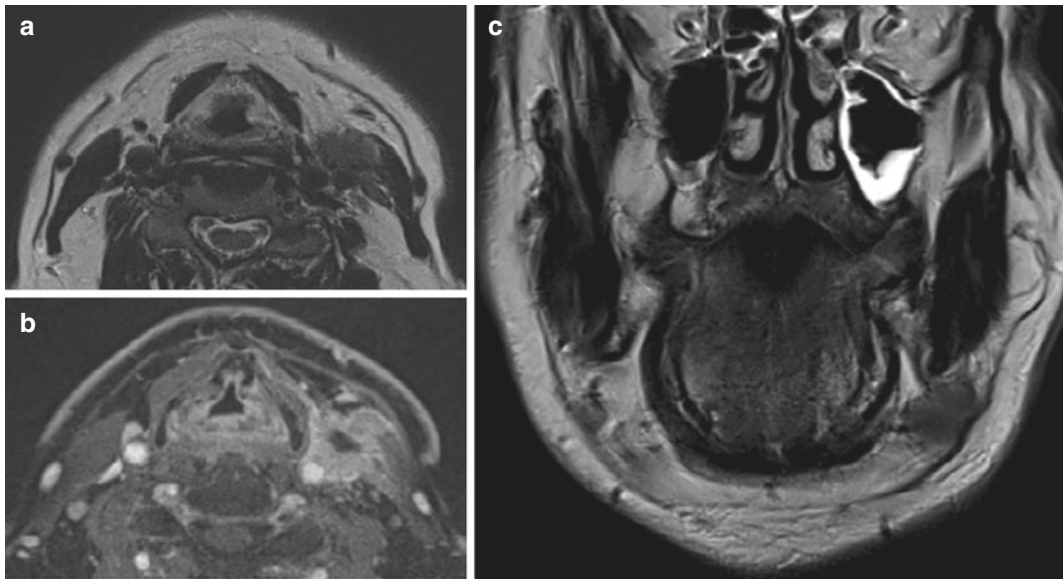

Fig. 4.9 Nodal metastasis with ENE+. (**a**, **b**) Loss of fatty plane with infiltration of SCM muscle and thrombosis of jugular vein. (**c**) Loss of fatty plane with infiltration of platysma muscle

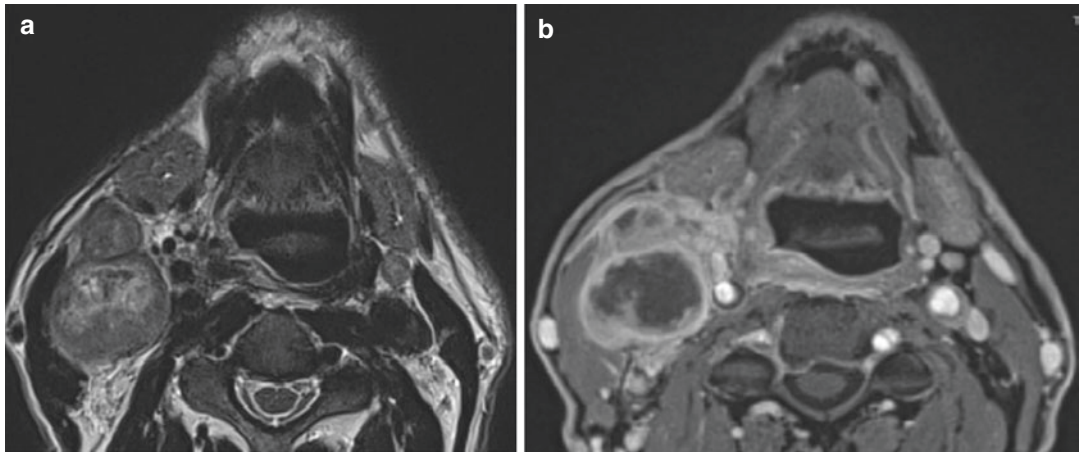

Fig. 4.10 Nodal metastasis from oropharynx carcinoma with round shape and central necrosis. (**a**) T2w image. (**b**) 3D T1w post-contrast image

often, metastatic lymph nodes of the head and neck region can present phenomena of central necrosis and cystic appearance, calcifications, or hyper-enhancement. Regardless of nodal size, the presence of intranodal necrosis (Fig. 4.10) should be considered pathologic and is reported to be present in one-third of all metastatic nodes [47].

Cases of cystic lymph nodes are more likely to have oropharyngeal (HPV-associated HNSCC) or thyroid (papillary carcinoma) origin. Calcified lymph nodes are most commonly present with thyroid carcinoma; other causes of nodal calcification are mucinous adenocarcinoma, treated lymphoma, treated or untreated HNSCC, and tuberculosis. Intranodal necrosis may be differentiated in US as a cystic ill-defined echolucent area within the nodes, the most common form of intranodal necrosis, and coagulation necrosis as an echogenic focus within lymph nodes but not continuous with the surrounding fat and that does not produce acoustic shadowing [48]. With CT, necrosis is identified as a focus of hypodensity with water attenuation density (10–25 HU) with an enhancing post-contrast rim. With MR, necrotic areas are defined as a focus of intranodal high signal intensity on T2-weighted imaging that corresponds to an intranodal nonenhancing area in contrast-enhanced T1-weighted imaging. Calcifications are better identified on US as punctuated echogenic foci with acoustic shadowing and on CT as hyperdense foci on pre-contrast scan.

Another aspect of inhomogeneity is vascular alterations that occur in metastatic lymph nodes. With CT and MR, metastatic adenopathy can show an increased vascularity, especially with specific histologic entities as thyroid carcinoma or melanoma, but it should be noted that a variety of conditions can demonstrate lymph node enhancement as infectious conditions or post-chemoradiotherapy. Doppler US is a very accurate method to detect vascular nodal anomalies; normal lymph nodes demonstrate hilar vascularity, while metastatic nodes show mixed vascularity both from hilum and from periphery. The presence of pericapsular vessels is a common appearance of metastatic nodes, and it is related to tumour infiltration in which tumour cells produce tumour angiogenic factor (TAF). Usually, reactive lymphadenopathy shows hilar vascularity or absent vascularity.

With US, it is also possible to distinguish different internal textures of lymph nodes reflecting in a different echogenicity. They are defined as hypo- or hyperechogenicity in contrast to the echogenicity of the surrounding muscle structures. Laterocervical lymph node metastases can be both hypoechogenic (lymphoma, HNSCC) and hyperechogenic (thyroid carcinoma, HNSCC).

4.5.2.4 Size

The classification according to the size of lymph nodes in the neck-head region can be confusing; in the literature, there are different studies on the cut-off of the laterocervical lymph nodes. However, the 10 mm shot-axis cut-off for the lymph node levels I–VII and the 8 mm short-axis cut-off for the remaining lymph nodes (retropharyngeal, nuchal, etc.) show a higher sensitivity [49, 50]. Due to the low specificity of this parameter, reactive lymph nodes (as ones secondary to infections) may show an increase in size, particularly in submandibular, upper jugular lymph nodes and in younger patients. Consequently, this parameter should be evaluated by looking for other ancillary signs.

4.5.2.5 Lymphatic Drainage

When suspicious nodes were located in the drainage pathway of the primary tumour, radiographic suspicion increased. Cervical lymph nodes should be classified on the basis of the system devised by the American Head and Neck Society and the American Academy of Otolaryngology-Head and Neck Surgery (Table 4.1).

In the majority of head and neck cancers (66.7%), the jugulodigastric node represents the sentinel node by way of internal jugular and deep

Table 4.1 Classification of nodal levels and drainage sites

Nodal levels	Landmarks	Drainage sites
I: IA—submental nodes, IB—submandibular nodes	Above the hyoid, below the mylohyoid muscle, anterior to the posterior edge of the submandibular gland IA: Between the medial margins of the anterior bellies of the digastric IB: Posterior and lateral to the medial edge of the anterior belly of the digastric	Nose and paranasal sinuses, lips, anterior oral cavity
II: upper jugular—IIA: upper internal jugular nodes, IIB: upper spinal accessory nodes	Below the skull base, above the hyoid, anterior to the posterior edge of the SCM, posterior to the posterior edge of the submandibular gland IIA: Posterior to the internal jugular vein/attached to the vein IIB: Posterior to the internal jugular vein/separate from the vein	Posterior oral cavity, oropharynx, supraglottic larynx, parotid gland
III: Mid-jugular	Below the lower body of the hyoid bone, above the lower margin of the cricoid, anterior to the posterior edge of the SCM, lateral to the medial margin of the common carotid artery/internal carotid artery	Hypopharynx, glottic, subglottic
IV: Lower jugular	Below the lower margin of the cricoid, above the clavicle, anterior and medial to the posterior edge of the SCM, lateral to the common carotid artery	Cervical oesophagus, subglottic, thyroid
V: VA, VB	Below the skull base, above the clavicle, anterior to the anterior edge of the trapezius, posterior to the posterior edge of the SCM VA: Above the lower margin of the cricoid VB: Below the lower margin of the cricoid	Skin carcinomas of the occipital scalp or neck, nasopharynx
VI	Below the hyoid, above the top of the manubrium, medial to the common carotid arteries/internal carotid arteries	Cervical oesophagus, subglottic, thyroid
VII	Below the top of the manubrium, medial to the left and right common carotid arteries	Cervical oesophagus, subglottic, thyroid

cervical lymphatic drainage. The first point of afferent drainage from the face, mouth, pharynx, and tonsils, the jugulodigastric node is the highest of the level II nodes and is located adjacent to the angle of the mandible. This node is commonly affected by tumours from the oral cavity and oropharynx. Tongue-based tumours, in some instances, can bypass the jugulodigastric and other level II nodes and spread directly to an ipsilateral low level III or IV node called the jugulo-omohyoid node. Thus, in the setting of tongue carcinoma, this node is another example of a sentinel node.

4.6 Advanced Imaging

4.6.1 Elastography

Ultrasound elastography provides information about the stiffness of the tissue by measuring the degree of strain on the tissue. Metastatic lymph nodes show an increase of stiffness and the level of suspicion for malignancy increases as the tissue hardens. During real-time ultrasound elastography, stiff components of 50% to less than 90% and 90% or greater of target lesion represent the class of suspicious for malignancy [51]. Ultrasound elastography showed an accuracy of 83.3%, sensitivity of 82.4%, and specificity of 84.6%; it should be helpful for detecting nodal metastasis of head and neck and can be safely used as a support technique to improve diagnostic performance of ultrasound of head-neck lymph nodes [52].

4.6.2 DWI-MRI

Diffusion-weighted MRI (DW-MRI) is a functional technique that measures the motion of water molecules in the extracellular, extravascular space, based on Brownian motion. In metastatic nodes, the microstructural changes such as the decreased extracellular space, increased cellularity, and higher nuclear-to-cytoplasmic ratio result in limited motion of water molecules and are represented as an area of hyperintensity on DWI and low signal intensity on the corresponding ADC map. DWI is a promising imaging technique to detect early metastatic lymph nodes. Vandecaveye et al. [53] showed that apparent diffusion coefficient (ADC) had 84% sensitivity and 94% specificity on a 1.5-T system, and Barchetti et al. [54] showed the ADC values of 97% sensitivity and 93% specificity on a 3-T system, in contrast to Lim et al. [55] who found no differences in ADC values between small metastatic and benign lymph nodes. Currently, DWI can be used as an additional tool in the detection of pathological lymph nodes and can be useful in 'uncertain' cases.

4.7 Preoperative Imaging for Thyroid Cancer Surgery

The success of thyroid cancer surgery relies on accurate preoperative imaging evaluation, which allows complete resection of the primary tumour and pathological lymph nodes. Ultrasound is still the most important imaging modality in the evaluation of thyroid cancer and should be used to evaluate both the primary cancer and all cervical lymph node compartments. Affected lymph nodes may be diagnosed according to size, shape, echogenicity, vascular pattern, loss of hilar structure, and presence of calcifications. Ultrasound-guided fine needle aspiration of affected lymph nodes can help in planning surgical radicality. Cross-sectional imaging may be considered in selected scenarios to better evaluate tumour invasion and/or inferiorly or posteriorly located lymph nodes. Functional imaging with positron emission tomography (PET) or PET/CT may have a selected role in patients affected by recurrent cancer with positive tumour markers and negative morphological imaging evaluation.

4.7.1 Introduction

The overall survival rates of thyroid cancer are high for most subtypes, exceeding 90%, though the risk of recurrence has been reported to be as high as 35% [56]. The majority of recurrent cancers are identified within the first 5 years after

diagnosis, representing persistent disease rather than recurrent one [57]. It is well known that the surgical radicality may be achieved through an accurate preoperative imaging evaluation, ensuring complete clearance of the primary tumour as well as pathological lymph node compartments. As stated in the Revised American Thyroid Association Management Guidelines for Patients with Thyroid Nodules and Differentiated Thyroid Cancer, ultrasound is the first-line imaging choice in the evaluation of thyroid cancer [58]. Furthermore, cross-sectional imaging has a role in selected scenarios to better evaluate tumour invasion and/or inferiorly or posteriorly located lymph nodes.

4.7.2 Preoperative Imaging Examination

According to the last update of TNM staging system (Table 4.2a–c), an accurate preoperative eval-

Table 4.2 Staging classification of thyroid malignancy: (**a**) differentiated thyroid carcinoma, (**b**) anaplastic thyroid carcinoma, and (**c**) medullary thyroid carcinoma

AJCC stage	Age	Stage	(a) Differentiated thyroid cancer
I	Younger than 55 years	Any T Any N M0	Any size with or without spread to lymph nodes (any N) and no distant metastasis (M0)
	OR		
	55 years or older	T1 N0 or NX M0	Any small tumour (<2 cm) with no spread to lymph nodes (N0) and no metastasis (M0)
	OR		
	55 years or older	T2 N0 or NX M0	The cancer is larger than 2 cm across but no larger than 4 cm and confined to the thyroid (T2) It has not spread to nearby lymph nodes (N0) or to distant sites (M0)
II	Younger than 55 years	Any T Any N M1	Any tumour (any T) with any metastasis (M1) regardless of whether it has spread to the lymph nodes (any N)
	OR		
	55 years or older	T1 N1 M0	The cancer is no larger than 2 cm across and confined to the thyroid (T1) with spread to nearby lymph nodes (N1) and no metastasis (M0)
	OR		
	55 years or older	T2 N1 M0	The cancer is larger than 2 cm across but no larger than 4 cm and confined to the thyroid with spread to nearby lymph nodes (N1) and no distant metastasis (M0)
	OR		
	55 years or older	T3a or T3b Any N M0	The cancer is larger than 4 cm but confined to the thyroid (T3a) or it has grown into the strap muscles around the thyroid (T3b), regardless of whether it has spread to the lymph nodes (any N). It has not spread to distant sites (M0)
III	55 years or older	T1/2/3 N1a M0	Any localized tumour (T1, T2, or T3) that has spread to the central compartment of lymph nodes (N1a) but has not metastasized (M0)
IVA	55 years or older	T4a Any N M0	The tumour has spread beyond the thyroid to nearby soft tissues, larynx, trachea, oesophagus, or recurrent laryngeal nerve, regardless of whether it has spread to the lymph nodes (any N). It has not spread to distant sites (M0)
IVB	55 years or older	T4b Any N M0	Tumour that has spread beyond nearby structures (T4b), regardless of spread to lymph nodes (any N), but no distant spread (M0)
IVC	55 years or older	Any T Any N M1	The cancer is of any size (any T) and might or might not have spread to nearby lymph nodes (any N) It has spread to other parts of the body, such as distant lymph nodes, internal organs, and bones (M1)

Table 4.2 (continued)

AJCC stage	Stage	(b) Anaplastic thyroid cancer
IVA	T1, T2 or T3a N0 or NX M0	The cancer is of any size but confined to the thyroid (T1, T2, or T3a) It has not spread to nearby lymph nodes (N0) or to distant sites (M0)
IVB	T1, T2, or T3a N1 M0	The cancer is of any size but confined to the thyroid (T1, T2, or T3a). It has spread to nearby lymph nodes (N1) It has not spread to distant sites (M0)
	OR	
	T3b Any N M0	The cancer is of any size and has grown into the strap muscles around the thyroid (T3b) It might or might not have spread to nearby lymph nodes (any N). It has not spread to distant sites (M0)
	OR	
	T4 Any N M0	The cancer is of any size and has grown extensively beyond the thyroid gland into nearby soft tissues of the neck or back toward the spine or into nearby large blood vessels It might or might not have spread to nearby lymph nodes (any N). It has not spread to distant sites (M0)
IVC	Any T Any N M1	The cancer is of any size (any T) and might or might not have spread to nearby lymph nodes (any N) It has spread to other parts of the body, such as distant lymph nodes, internal organs, and bones (M1)
AJCC stage	**Stage**	**(c) Medullary thyroid cancer**
I	T1 N0 M0	The cancer is 2 cm or smaller and confined to the thyroid (T1). It has not spread to nearby lymph nodes (N0) or to distant sites (M0)
II	T2 N0 M0	The cancer is larger than 2 cm but no more than 4 cm across and confined to the thyroid (T2). It has not spread to nearby lymph nodes (N0) or to distant sites (M0)
	OR	
	T3 N0 M0	The cancer is larger than 4 cm and confined to the thyroid or any size and growing outside of the thyroid but not involving nearby structures (T3). It has not spread to nearby lymph nodes (N0) or to distant sites (M0)
III	T1, T2, or T3 N1a M0	The cancer is of any size and might be growing outside of the thyroid but not involving nearby structures (T1, T2, T3). It has spread to lymph nodes in the neck (pretracheal, paratracheal, prelaryngeal, or upper mediastinal) (N1a) but not to other lymph nodes or to distant sites (M0)
IVA	T4a Any N M0	The cancer is of any size and has grown beyond the thyroid gland into nearby tissues of the neck, such as the larynx (voice box), trachea (windpipe), oesophagus (tube connecting the throat to the stomach), or nerve to the larynx (T4a) It might or might not have spread to nearby lymph nodes (any N). It has not spread to distant sites (M0)
	OR	
	T1, T2, or T3 N1b M0	The cancer is of any size and might be growing outside of the thyroid but not involving nearby structures (T1, T2, T3) It has spread to certain lymph nodes in the neck such as cervical or jugular nodes (N1b). It has not spread to distant sites (M0)
IVB	T4b Any N M0	The cancer is of any size and has grown either back toward the spine or into nearby large blood vessels (T4b) It might or might not have spread to nearby lymph nodes (any N). It has not spread to distant sites (M0)
IVC	Any T Any N M1	The cancer is of any size and might have grown into nearby structures (any T) It might or might not have spread to nearby lymph nodes (any N). It has spread to distant sites such as the liver, lung, bone, or brain (M1)

uation is mandatory for planning the best treatment. The aims of preoperative sonographic assessment in patients affected by or with suspected thyroid cancer are to evaluate the primary tumour and to detect pathological lymph nodes in the central (level 6: pretracheal, right paratracheal, and left paratracheal), lateral (levels 2, 3, and 4: jugular), and posterior (level 5: posterior to sternocleidomastoid muscle) neck compartments, ensuring a compartment-oriented surgical resection.

4.7.3 Ultrasound Evaluation of Primary Tumour

Most of the thyroid nodules are incidental findings discovered by imaging studies unrelated to the thyroidal gland [59]; being found in up to 68% of normal population, most of them are asymptomatic, showing benign appearance, and will never develop into a cancer. The aim of a first-line ultrasound evaluation of thyroid nodules is to differentiate benign nodules from suspicious or malignant ones requiring further management; about that, fine needle aspiration (FNA) plays a pivotal role in this process, but it needs to be performed in a selective way, rather than systematic procedure, regardless of the nodule size or appearance [60]. It is mandatory to evaluate the primary tumour assessing size, location, margins, multifocality, and local invasion (Fig. 4.11). Further, it is important to report postero-medially located tumour beside the recurrent laryngeal nerve may affect patient preoperative evaluation and surgical approach. Local invasion of strap muscles is quite common and usually does not affect resection strategy significantly; nevertheless, visceral or vascular invasion, sonographically depicted by a blurry or indistinct deep margin, may require cross-sectional evaluation and surgical approach changes. Furthermore, additional tumour foci must be evaluated, since contralateral lesions may result in the need to exclude positive contralateral lymph nodes [61, 62].

Fig. 4.11 Effaced fatty tissue in the tracheoesophageal groove where the recurrent laryngeal nerve courses

4.7.4 Risk Stratification Systems

Thyroid gland ultrasound evaluation of the risk of malignancy plays a central role in patients with nodules, with the aim of selecting lesions that should have a fine needle aspiration (FNA) performed. According to the key role of thyroid US in the management of patients affected by nodules, several associations, such as the European Thyroid Association, the Korean Society of Thyroid Radiology, the American Thyroid Association, the American Association of Clinical Endocrinologists, the American College of Endocrinology, and the Italian Associazione Medici Endocrinologi, have issued recommendations for US risk stratification of thyroid nodules [63, 64]. Two of the most used ultrasound-based classification systems for thyroid nodules are the American College of Radiology (ACR) TIRADS and European (EU) TIRADS. In 2015, an American committee convened by the ACR presented a system for approaching the thyroid nodules and the proper lexicon for reporting. The white paper was titled ACR Thyroid Imaging, Reporting and Data System (ACR TI-RADS) [65, 66].

The ACR-TIRADS is a scoring system, based on the US features of a given nodule, according to its composition, echogenicity, shape, margin, and echogenic foci; the higher the score, the greater the risk of malignancy, which would imply performing FNA for a better characterization of the lesion. Based on literature evidences and on the American Association of Clinical Endocrinologists, American Thyroid Association, and Korean guidelines, the European Thyroid Association (ETA) states guidelines and a risk stratification system, establishing a US lexicon, a

report template, and definitions of benign and low-, intermediate-, and high-risk nodules, with the estimated risks of malignancy in each category, which was named European Thyroid Imaging and Reporting Data System (EU-TIRADS) [67]. Recommendations for biopsy or US follow-up are based on the nodule's TI-RADS level and its maximum diameter. Both the EU-TIRADS and ACR-TIRADS are practical and useful classification systems recently developed. They share common characteristics, but also some differences; categorization differences are shown in Table 4.3, and different managements are described in Table 4.3. Both systems also recommend checking cervical lymph nodes, especially in the intermediate- and high-risk nodule, and perform FNA in the presence of suspicion feature, such as round shape, loss of echogenic hilum, peripheral disorganized flow, heterogeneity, and gland-like echogenicity within the node.

Table 4.3 Ultrasound characteristic for TIRADS classification of thyroid nodules

Category	**US score**	**Cancer risk**
ACR-TIRADS 1: Benign	0 points	0.3%
ACR-TIRADS 1: Not suspicious	2 points	1.5%
ACR-TIRADS 1: Mildly suspicious	3 points	4.8%
ACR-TIRADS 1: Moderately suspicious	4 to 6 points	9.1%
ACR-TIRADS 1: Highly suspicious	7 points or more	35%
Category	**US features**	**Cancer risk**
EU-TIRADS 1: Normal	No nodules	–
EU-TIRADS 2: Benign	Colloidal cyst, entirely spongiform nodule	Close to 0%
EU -TIRADS 3: Low risk	Ovoid, smooth, iso/hyperechoic, no features of high suspicion	2–4%
EU-TIRADS 4: Intermediate risk	Ovoid, smooth, mildly hypoechoic, no features of high suspicion	6–17%
EU-TIRADS 5: High risk	At least one of the following features of high suspicion: • Non-oval/round shape • Irregular margin • Microcalcifications • Markedly hypoechoic	26–87%
Classification	**ACR-TIRADS**	**EU-TIRADS**
Normal gland	–	EU-TIRADS 1
Benign (cystic/spongiform)	TR1	EU-TIRADS 2
Not suspicious (mixed cystic/solid)	TR2	–
Mildly suspicious/low risk	TR3	EU-TIRADS 3
Moderately suspicious/intermediate risk	TR4	EU-TIRADS 4
Highly suspicious/high risk	TR5	EU-TIRADS 5
TIRADS 1	No F/U-no FNA	–
TIRADS 2	No F/U-no FNA	No FNA unless compressive
TIRADS 3	F/U ≥ 1.5 cm FNA ≥2.5 cm	FNA >2 cm
TIRADS 4	F/U ≥1.0 cm FNA ≥1.5 cm	FNA >1.5 cm
TIRADS 5	F/U ≥0.5 cm FNA ≥1.0 cm	FNA >1.0 cm F/U or FNA <1.0 cm

A recent published article compared in a prospective way five of the most used classification systems (ACR, ATA, AACE/ACE/AME, EU-TIRADS, and K-TIRADS), demonstrating that all of them have a very reliable discriminatory capacity, reducing the number of unnecessary biopsies, being particularly higher in the case of ACR. The article stated that ACR showed a better overall performance, classifying half of the biopsies as unnecessary, with a false-negative rate of 2% [68]. Another recent study published in 2018 assessed the interobserver variability of the classification systems AAC/ACE/AME, ACR, ATA, EU-TIRADS, and K-TIRADS and the interobserver concordance in the indication of FNA biopsy. When selecting the nodules for which FNA biopsy has to be performed, the interobserver agreement is substantial to almost perfect [69].

Another recent study in 2018 was conducted to evaluate the temporal stability of initial risk calculated with five systems and determine whether the risk class increase during the follow-up is indicative of malignancy. It was demonstrated that benign nodules tend to stay stable in time, and changes that require biopsies are rare. Development of new nodules is frequent, but few of them (less than 5%) are classified as a high risk. So, this means that benign nodules could be followed in a secure way with less intense surveillance protocols [70].

Finally, the ACR-TIRADS and EU-TIRADS are very good and useful systems of malignancy risk stratification. Due to the differences between both categorization systems, it is recommended to use one of them and clearly specify the used one in the radiological report to avoid confusion and allow a proper patient management.

4.8 Ultrasound Findings in Benign and Malignant Lymph Nodes

Metastatic papillary thyroid carcinoma (PTC) affects central and lateral lymph nodes in up to 70% of cases [71]. Pathological lymph node involvement may be observed upon the first examination or in follow-up evaluation in cases of recurrence. Ultrasound is approved to be the first-line imaging modality for lymph node assessment in both scenarios [72]. The sensitivity of ultrasound in detecting abnormal lymph nodes varies widely in the literature, ranging from 25% to 60% for the central neck and from 70% to 95% for the lateral neck [73]; further, the specificity of ultrasonography in detecting PTC-affected lymph nodes is high, ranging from 80% to 95% in both the central and lateral neck [74]. As the neck compartments have multiple lymph nodes (100–200), any of which could increase its dimension related to benign or malignant disease, it is crucial to know the ultrasound findings that help to distinguish benign lymph nodes from malignant. The evaluation of lymph nodes for assessing the presence of malignancy must be competent to identify the features of a benign lymph node. Enlarged nodes can be the expression of a benign reactive or malignant process. Benign lymph nodes usually are oval in morphology, with a hyperechoic central hilum and unipolar vascularization at colour Doppler examination. Lack of the hilum may represent a sign of tumour invasion. Nevertheless, the hilum may not always be easily identified by ultrasonography in a benign lymph node; the specificity for predicting the presence of cancer when the hilum is not displayed is 29% according to Lebolleux et al. [75].

Lymph node location is another important factor when searching for potential metastatic involvement. As previously stated, cervical lymph nodes are grouped into six levels. When lymph node dissections are performed, pathological lymph nodes related to thyroid cancer are most frequently identified in ipsilateral level 6 (prevalence 50–70%), followed by ipsilateral levels 2, 3, and 4 (prevalence 30–45%) [76]. In the presence of primary tumours <1 cm, contralateral level 6 is less commonly affected (prevalence 5–25%), and contralateral levels 2, 3, and 4 are rarely affected (prevalence 5–14%) [77]. Although the size of lymph nodes >1 cm in maximum diameter has typically been considered more likely related to tumour invasion, many benign or reactive nodes will exceed this size while remaining fusiform in shape. Conversely,

malignant lymph nodes have the tendency to become rounded in shape, and this helps to distinguish them from benign nodes (Fig. 4.11). The shortest diameter of the lymph node can be a feature that helps in predicting the likelihood of tumour involvement. So, comparing the long and short axes of the lymph node (Solbiati index), a ratio below 2.0 becomes suspicious for the presence of malignant involvement [78].

Just as with thyroid nodules, microcalcifications are a highly specific feature; a lymph node containing microcalcifications in a patient affected by PTC or MTC should be suspected to be positive for malignant involvement. The echogenicity is another key feature that can also be useful for detecting metastatic lymph nodes. Benign lymph nodes typically are uniformly hypoechoic with hyperechoic central hilar structure; however, lymph nodes affected by malignant process may appear hyperechoic, exhibit the same echogenicity of the primary tumour, or even exhibit cystic changes to the point of total cystic replacement with complex structure.

The last but not least feature helping in differentiating malignant from benign lymph nodes is the peripheral and disorganized vascularity. The vascular flow of a lymph node can be assessed by the conventional colour and power Doppler or by the recently developed imaging technique named superb microvascular imaging (SMI), which aims to visualize low-velocity and small-diameter blood vessel flow [79].

Benign lymph nodes exhibit typical unipolar vascularization in the hilum, while tumour invasion stops this flow [80], showing peripheral and disordered flow pattern throughout the node.

4.9 Ultrasound in Presurgical Planning

4.9.1 Preoperative Ultrasound Role in Malignant Cytology

Mapping of bilateral lymph node compartments by using ultrasound should be performed routinely in the scenario of cytologic evidence of carcinoma (positive fine needle aspiration), for ensuring a surgical radicality of the primary tumour as well as a compartment-oriented surgical resection of affected lymph nodes. Surgeons may decide to repeat the US evaluation immediately prior to resection in order to have an anatomic map. After the FNA confirmation of malignancy of the primary thyroid lesion, FNA of lymph nodes which present suspicious features at US examination should be performed to provide strong justification for adding lymph node resection to initial surgery. Preoperative ultrasound may provide insight into the need for further imaging prior to surgery. The US finding of an indistinct margin between the thyroid lesion and nearby structures may prompt cross-sectional imaging. Furthermore, adenopathy in levels 6 and 4 requires cross-sectional imaging of substernal or infraclavicular located lymph nodes that may be difficult to assess by ultrasonography.

4.9.2 Preoperative Ultrasound Role in Indeterminate or Suspicious Cytology

Subcategories of indeterminate cytology include ‘atypia of undetermined significance’ or ‘follicular lesion of undetermined significance’ (malignancy risk 5–15%), ‘follicular neoplasm’ or ‘suspicious for follicular neoplasm’ (malignancy risk 15–30%), and ‘suspicious for malignancy’ (malignancy risk 60–75%) [81]. Although a great number of these patients undergo surgical resection, the majority of lesions classified as indeterminate are ultimately diagnosed as benign [82]. There are several studies exploring the utility of ultrasound to predict the risk of malignancy in patients presenting indeterminate FNA cytology lesion. Hypoechogenicity, increased vascularity, irregular margins, microcalcifications, and taller-than-wide shape are all features related to an increased risk of malignancy [58]. These ultrasound features may be used to predict malignancy risk in FNA cytology indeterminate nodules [83].

Ultrasound evaluation of the central and lateral lymph node compartments may help the cli-

nician in the presurgical planning for cytologically indeterminate lesions. When abnormal central (level 6) or lateral lymph nodes (levels 2, 3, and 4) are identified, FNA cytology should be performed on at least one of these nodes. Further, to find thyroid cells within suspected lymph nodes, confirm the diagnosis of metastatic thyroid cancer, altering significantly the surgical management of the patient with indeterminate thyroid cytology.

4.10 Ultrasound in Revision Surgery

Ultrasound is an important imaging modality for thyroid cancer follow-up and facilitating the detection, localization, and planning of revision surgery in the setting of recurrent/persistent disease. In this scenario, post-surgical inflammation, scarring, and inflammatory adenopathy represent known limitations, advising a 6-month time interval after surgery in order to favour the resolution of alterations resulting from the surgical manipulation of the neck compartments. There are some exceptions arising from incomplete surgery and/or insufficient compartment-oriented nodal resection in the initial surgery. Follow-up examination of thyroid cancer patients should be annually performed [58]. Suspicious lymph nodes should be subjected to FNA cytology in the case where further surgery is planned and lymph nodes exceed 8 mm in diameter.

The scenario of suspected persistent or recurrent thyroid malignancy needs FNA cytology of any tissue or abnormal adenopathy located in the central neck compartment and/or thyroid bed. A cytologic diagnosis would justify a high-risk revision surgery. US abnormal and anatomically hazardous lymph nodes represent exception to these rules, recommending revision surgery regardless of FNA cytology. In this setting, to perform serum thyroglobulin aids clinical decision-making. In thyroid cancer surveillance, it is mandatory to bear in mind any US findings of the primary pathology, surgical report, and TNM staging; in fact, ipsilateral lymph node recurrences occur in up to 25% of patients with primary diagnosis of positive lymph nodes. In patients affected by locally invasive malignancy, the main concern is the risk of local recurrence, requiring the support of cross-sectional imaging.

4.11 Cross-Sectional Imaging

Ultrasound is the first-line modality for an accurate presurgical thyroid and cervical lymph node examination because it is highly available, is time-saving, ensures detailed high-resolution findings, is ionizing radiation free, and aids the characterization of indeterminate nodules guiding fine needle aspiration procedure [84]. Some US limitations, such as the assessment of deep structures and nearby acoustically shielded by air/and or bone, limits the use of cross sectional imaging in preoperative thyroid cancer evaluation. Other circumstances in which computed tomography (CT) or magnetic resonance imaging (MRI) may play an additional role include (1) presence of an invasive primary tumour, (2) presence of a bulky primary tumour or nodal disease partially investigated with ultrasonography, and (3) clinical settings suspected for advanced disease (e.g. vocal cord paralysis, progressive dysphagia, or respiratory symptoms). On the other hand, the increased use of CT and MRI implies a great number of thyroid incidentalomas, becoming a growing problem. The decision to include thyroid nodule in CT or MR report is difficult in the absence of signs of extrathyroidal extension, because there are no clear findings that allow a reliable identification of malignant lesions [85]. Some studies have reported added value performing diffusion-weighted imaging because benign nodules have a higher apparent diffusion coefficient value, even if actually the preferred modality for workup is still ultrasound [86].

4.11.1 Cross-Sectional Imaging Evaluation of the Primary Tumour

Ultrasound features of the thyroid malignancy suggestive for local invasion and/or mediastinal involvement necessarily require cross-sectional imaging. Chest CT aids in determining the caudal

extent of the disease and the involvement of great vessels and tracheobronchial structures. These findings influence surgical planning by implying the need for sternotomy and/or tracheal resection/reconstruction. The CT of neck structures with contrast medium is useful in defining the involvement of nearby structures in the setting of extrathyroidal extension. Hence, the support of cross-sectional imaging is recommended in preoperative evaluation of clinically suspected scenario, though preoperative screening for distant metastasis is actually not performed for differentiated thyroid cancers [83].

Further, communication with the clinician plays an important role before performing a contrast CT scan, because the free iodine load due to contrast medium administration interferes with thyroidal iodine uptake for at least 6–8 weeks [87], resulting in not being able to use diagnostic thyroid scintigraphy and/or radioiodine ablation for 2–6 months depending on the institution [88]. Conversely, MRI contrast (gadolinium chelate) does not interfere with iodine thyroidal uptake, offering a better contrast resolution and better tissue differentiation.

Except in cases of patients affected by anaplastic carcinoma, the routine treatment for thyroid carcinoma includes total or near-total thyroid resection, central lymphadenectomy, and possible radioiodine ablation [83]. Surgical approach limited to lobectomy may be reserved for solitary malignancy less than 10 mm; conversely, complete thyroid gland resection and radioiodine ablation are preferred in the presence of small multifocal tumours. However, the diagnosis of multifocal tumour cannot be based on CT or MRI approach; therefore, presurgical imaging evaluation starts with ultrasound to identify multifocal disease and pathological nodes, continuing with CT and/or MRI if extrathyroidal extension is suspected. The assessment of local invasion, according to the AJCC/UICC tumour (T) staging, accounts for four groups of structures: the airway and nerves centrally, the carotid arteries laterally, the prevertebral space posteriorly, and the mediastinum inferiorly. MRI and CT have similar accuracy for predicting local invasion of the oesophagus, trachea/larynx, and RLN [89]. The main CT/MRI sign suggestive for tracheal and oesophageal involvement is a circumferential ≥180° contact or irregular wall or lumen or intraluminal mass, though it is more difficult to evaluate the oesophageal parietal lining because it is generally not distended with air and is more compressible than the trachea [88, 89].

Another important sign of extrathyroid extension is represented by effaced fatty tissue in the tracheoesophageal groove where the recurrent laryngeal nerve courses (Fig. 4.11) (RLN), predicting a possible nerve involvement [90]. Further, dysfunction of vocal cord, highlighted by a dilated right laryngeal ventricle and anteromedial positioning of the right arytenoid cartilage, may represent an imaging sign or RLN invasion.

Extrathyroidal extension to vascular and prevertebral space results in T4b disease (Table 4.1). Generally, these findings are better appreciated on cross-sectional imaging and preclude the patient from curative surgery. A study published by Seo et al. reported that encasement of 180 or more degree of the common carotid artery and internal jugular vein is a specific sign of vascular involvement, although vascular compression or effaced fatty tissue is a further criterion to keep in mind [88].

MRI prevertebral muscle evaluation may detect effaced retropharyngeal fat plane and/or T2 intensity change and/or enhancement as possible signs of muscle invasion. Further, detecting anomalous anatomic structures at cross-sectional imaging is an important step in the planning of primary surgery; an example is the presence of non-recurrent inferior laryngeal nerve (NRILN). A radiologist could suggest this anatomic variant when there is an aberrant right SCA [50].

4.11.2 Cross-Sectional Imaging in the Assessment of Cervical Lymph Nodes

The most common thyroid malignancy affecting lymph nodes is papillary and medullary subtype, whereas local invasion and distant metastases to

the bone and lung are more common in follicular carcinoma, which rarely affects lymph nodes. Cross-sectional CT or MR imaging may be used as a complementary examination to obtain a complete nodal evaluation when clinical and/or US raises suspicion of extensive nodal involvement. Indeed, the limited ultrasound evaluation of deep and/or acoustically shielded structures represents the strongest indication to use cross-sectional imaging in presurgical assessment. The American Thyroid Association has recently published the evidence that the prognostic value of nodal involvement in papillary thyroid carcinoma is related to the size and number of affected nodes and that extranodal extension is an independent factor of poor outcome [91]. Pathology specimens often demonstrate extracapsular extension in affected large nodes (>3 cm). Affected nodes located in the inferior aspects of level 4 and 6 on US in patients with thyroid malignancy may take advantage from cross-sectional imaging of the lower neck/upper chest to assess mediastinal lymph nodes, such as the deep tracheoesophageal groove and infraclavicular space (Fig. 4.12), resulting in altered surgical approach.

In a patient affected by a nodal mass, the presence of cystic components, calcification, proteinaceous (thyroglobulin results in high T1 signal) or haemorrhagic content, and intense enhancement must suggest a thyroid primary [92].

Therefore, it is mandatory not to define all cystic lesions of the neck as congenital cysts, especially in young adults, but to consider them as suspected secondary lesions of thyroid malignancy until proven otherwise. Nodal staging is better performed if the radiologist is aware of the common sites of lymph node involvement. The most frequent level involved with thyroid malignancy is the central compartment (level IV) and lateral nodal stations (levels II–IV) [93]. Prelaryngeal lymph node is the highest central compartment lymph node and its involvement in patients affected by papillary thyroid cancer is predictive of advanced nodal disease. The TNM staging system, according to the American Joint Committee on Cancer (AJCC)/Union for International Cancer Control (UICC), classified nodal stage as N1a if level VI pretracheal, paratracheal, and Delphian nodes are affected and N1b if there is malignancy involvement of unilateral/bilateral cervical nodes or superior mediastinal nodes (level VII) (Table 4.1). N1b stage may preclude curative surgery or change operative approach; therefore, cross-sectional imaging may be indicated if there are US predictors of mediastinal involvement such as lateral nodes or thyroid malignancy greater than 1.5 cm [93]. Not less important, regarding nodal involvement, is the detection of skip nodal metastasis, occurring in up to 21% of cases of MTC [94].

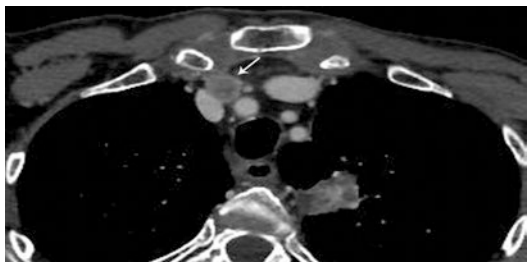

Fig. 4.12 Cross-sectional imaging of the lower neck and upper chest to assess mediastinal lymph nodes, such as the deep tracheoesophageal groove and infraclavicular space

4.11.3 Cross-Sectional Imaging Assessment in Revision Surgery

In previously treated patients, cross-sectional imaging should be taken into account in those suffering from dysphagia, respiratory symptoms, hoarseness, or vocal cord paralysis for assessment of invasive central neck disease. Recurrent or residual differentiated thyroid tumours have to be suspected according to serum thyroglobulin level increase; in this setting, a neck US and/or 131I or 123I whole-body imaging are suggested. When the latter results to be negative (50–80% of patients), a progression with dedifferentiated thyroid cancer has to be excluded [91]. In such a scenario, MRI or PET/CT has a role in detecting recurrent disease. MRI can be readily performed in suspected thyroid recurrence, even if it is not dedifferentiated, because it does not require iodinated contrast and allows to identify nodal

involvement with high protein content from colloid, thyroglobulin, and haemoglobin products [94]. In the setting of prior lateral and central neck dissection, it becomes mandatory to carefully exclude the retropharyngeal nodal disease [94].

PET/CT has usually limited sensitivity in the detection of differentiated thyroid tumour, but it shows the tendency for FDG uptake according to the tumour progressive dedifferentiation and a more aggressive behaviour [94].

4.12 The Post-treatment Role of Radiology

Follow-up imaging in patients with a history of head and neck cancer is essential to assess response to treatment, although it is often difficult to interpret because of anatomic changes in the post-surgery and radiotherapy setting. Anatomic changes in the head and neck region are due to two types of complications; post-surgical complications include wound infection, abscess, fistula, flap necrosis, haematoma, chylous fistula, and seroma; postradiotherapy changes include mucosal necrosis, osteoradionecrosis, radiation-induced vasculopathy, radiation pneumonitis, radiation lung fibrosis, radiation-induced brain necrosis, and radiation-induced neoplasms.

Various imaging modalities, such as radiography, fluoroscopy, endoscopy, ultrasonography (US), computed tomography (CT), magnetic resonance imaging (MRI), single photon emission CT (SPECT), and dual-modality imaging with 2-(fluorine 18)-fluoro-2-deoxy-D-glucose (FDG) positron emission tomography (PET) with CT (PET/CT), are used to evaluate the post-treatment status in patients treated for head and neck cancer [95, 96].

In the literature, combined PET and CT imaging has been reported as a highly sensitive technique for detecting head and neck cancer recurrence in the post-treatment setting [96, 97], although PET can produce a high number of false positives if used too early from the start of radiation therapy (within 3 months of the start of treatment), because of post-radiation inflammation [98, 99].

Therefore, it is seen that MRI in diffusion sequences is a more useful tool at an early stage to differentiate tumour recurrence from normal post-treatment changes [98, 100, 101]. Resection of the neoplasm to be defined as curative must require extensive local excision with all-negative surgical margins; however, given the anatomic complexity of the head and neck, complex reconstructive techniques are often required to close the surgical defect, which can thus be classified into three types of flap reconstruction [95, 102, 103].

Local flap reconstruction involves repositioning by sliding the adjacent tissue. Pedicle flap reconstruction is performed by rotation of donor tissue to cover a defect, using the original vascular pedicle. Free flap reconstructive technique involves the transfer of vascularized tissue from local vessels, with anastomosis to the tissue defect using microvascular techniques. The more common types of free flaps used in the head and neck region are the rectus abdominis myocutaneous free flap, radial forearm free flap, lateral arm flap, anterior lateral thigh flap, iliac crest flap, and fibula free flap. The most frequently used pedicle flaps are the pectoralis major flap, latissimus dorsi flap, deltopectoral flap, trapezius flap, and platysma flap 105]. Myocutaneous flaps are initially depicted as a mass with soft-tissue attenuation and soft-tissue intensity, representing muscle [95, 102, 104]. They will gradually develop innervation atrophy, resulting in volume loss and fat replacement of the muscle [95, 102, 105].

An important radiologic sign to evaluate after reconstructive surgical treatment is the presence of clear boundaries between the flap and adjacent normal structures as an indication of benignity, especially at the upper and lower margins of the flap, where local recurrence most commonly occurs [95, 102, 105]. Imaging is essential for the evaluation of potential tumour recurrence deep within the reconstruction flap, as it often cannot be inspected or palpated clinically. Neoplastic recurrence typically recurs within the first 2 years after treatment. The most common sites of tumour

recurrence are at the soft-tissue level of the surgical bed and at the margins of the surgical site.

CT shows the recurrence as a slightly hyperattenuated infiltrating mass in a muscle-like manner. Therefore, if a suspicious mass has less attenuation than muscle, it is unlikely to be a neoplasm and it is often related to post-treatment oedema [95]. The main CT and MR imaging finding after neck dissection is the absence of resected tissues with cervical lymph nodes, which is more easily identified in patients undergoing radical neck dissection or a modified radical neck dissection [95]. Another imaging finding commonly seen after neck dissection is an area of soft-tissue attenuation surrounding the carotid sheath completely on CT [95, 103].

On MRI, this post-operative area shows low-to-intermediate signal intensity on T1- and T2-weighted MRI images, a result of scar fibrosis. The fat planes often become obliterated, making it more difficult to identify lymph node recurrence [103]. Typical findings of early radiotherapy reactions visible on CT and MRI are thickening of the skin and platysma, cross-linking of subcutaneous fat, oedema and fluid in the retropharyngeal space, increased volume of the major salivary glands, thickening and increased volume of the pharyngeal walls, and thickening of the structures of the larynx. Consequences of radiation therapy include atrophy of the salivary glands and thickening of the pharyngeal constrictor muscle, platysma, and skin [95, 103].

In the evaluation of tumour recurrence, MRI demonstrates that the tumour recurs as an infiltrating mass with intermediate-to-high T1-weighted signal intensity and T2-weighted signal intensity [95, 103, 105]. It is often difficult to make a differential diagnosis between neoplastic recurrence and a vascularized scar, i.e. early fibrosis, because such a scar appears as a soft-tissue mass with indefinite margins and enhancement as well as tumour recurrence on both CT and MRI [103]. In contrast, fibrosis produces retraction and decreased signal intensity on T2-weighted MRI images [106, 107]. The best technique for evaluating suspected tumour recurrence is to signal on diffusion-weighted MRI images with a decreased value for the apparent diffusion coefficient (ADC). The use of ADC has been reported to result in high sensitivity and specificity, with almost no overlap between tumour and nontumour tissue [100]. This low value of ADC is thought to be caused by the restriction of proton movement in the extravascular extracellular space secondary to tumour hypercellularity. On the other hand, necrosis, inflammation, and submucosal fibrosis after treatment show elevated values for ADC, a finding that correlates with increased interstitial space and low cell density [96, 98, 101].

Similarly to its use at the primary tumour site, diffusion-weighted MRI imaging is useful in characterizing persistently enlarged lymph nodes after treatment. In particular, lymph node recurrences or metastases have high signal intensity with a decreased value for ADC on diffusion-weighted MRI images [100].

References

1. Siegel RL, Miller KD, Jemal A. Cancer statistics, 2019. CA Cancer J Clin. 2019;69(1):7–34. https://doi.org/10.3322/caac.21551.
2. Aupérin A. Epidemiology of head and neck cancers: an update. Curr Opin Oncol. 2020 May;32(3):178–86. https://doi.org/10.1097/CCO.0000000000000629.
3. Michaud DS, et al. High-risk HPV types and head and neck cancer. Int J Cancer. 2014;135:1653–61. https://doi.org/10.1002/ijc.28811.
4. Stein AP, et al. Prevalence of human papillomavirus in oropharyngeal cancer: a systematic review. Cancer J. 2015;21:138–46. https://doi.org/10.1097/PPO.0000000000000115.
5. Isayeva T, Li Y, Maswahu D, Brandwein-Gensler M. Human papillomavirus in non-oropharyngeal head and neck cancers: a systematic literature review. Head Neck Pathol. 2012;6(Suppl 1):S104–20. https://doi.org/10.1007/s12105-012-0368-1.
6. Johnson DE, Burtness B, Leemans CR, et al. Head and neck squamous cell carcinoma. Nat Rev Dis Primers. 2020;6:92.
7. Glastonbury CM. Chapter 17: Head and neck squamous cell cancer: approach to staging and surveillance. In: Hodler J, Kubik-Huch RA, von Schulthess GK, editors. Diseases of the brain, head and neck, spine 2020–2023: diagnostic imaging. Cham: Springer; 2020.
8. Schlumpf MF, Haerle S. The current role of imaging in head and neck cancer: a clinician's perspective.

Swiss Med Wkly. 2014;144:w14015. Published 2014 Sept 25. https://doi.org/10.4414/smw.2014.14015.
9. Ong CK, Chong VF. Imaging of perineural spread in head and neck tumours. Cancer Imaging. 2010;10(1A):S92–8. Published 2010 Oct 4. https://doi.org/10.1102/1470-7330.2010.9033.
10. Gupta V, Demmy T. Lung metastases from head and neck cancer, diagnosis and management. In: Kountakis SE, editor. Encyclopedia of otolaryngology, head and neck surgery. Berlin: Springer; 2013. https://doi.org/10.1007/978-3-642-23499-6_40.
11. Tshering Vogel DW, Thoeny HC. Cross-sectional imaging in cancers of the head and neck: how we review and report. Cancer Imaging. 2016;16(1):20. Published 2016 Aug 3. https://doi.org/10.1186/s40644-016-0075-3.
12. Ferlay J, Shin HR, Bray F, Forman D, Mathers C, Parkin DM. Estimates of worldwide burden of cancer in 2008: GLOBOSCAN 2008. Int J Cancer. 2010;127:2893–917. https://doi.org/10.1002/ijc.25516.
13. Windon MJ, D'Souza G, Rettig EM, Westra WH, van Zante A, Wang SJ, Ryan WR, Mydlarz WK, Ha PK, Miles BA, Koch W, Gourin C, Eisele DW, Fakhry C. Increasing prevalence of human papillomavirus-positive oropharyngeal cancers among older adults. Cancer. 2018;124(14):2993–9. https://doi.org/10.1002/cncr.31385.
14. Fung SY, Lam JW, Chan KC. Clinical utility of circulating Epstein-Barr virus DNA analysis for the management of nasopharyngeal carcinoma. Chin Clin Oncol. 2016;5(2):18. https://doi.org/10.21037/cco.2016.03.07.
15. Pynnonen MA, Gillespie MB, Roman B, et al. Clinical practice guideline: evaluation of the neck mass in adults. Otolaryngol Head Neck Surg. 2017;157(2_Suppl):S1–S30. https://doi.org/10.1177/0194599817722550.
16. Taberna M, et al. Human papillomavirus-related oropharyngeal cancer. Ann Oncol. 2017;28(10):2386–98. https://doi.org/10.1093/annonc/mdx304.
17. Lewis JS Jr, et al. Human papillomavirus testing in head and neck carcinomas: guideline from the College of American Pathologists. Arch Pathol Lab Med. 2018;142(5):559–97. https://doi.org/10.5858/arpa.2017-0286-CP.
18. Glastonbury CM. Critical changes in the staging of head and neck cancer. Radiol Imaging Cancer. 2020;2(1):e190022. https://doi.org/10.1148/rycan.2019190022.
19. Zanoni DK, Patel SG. New AJCC: how does it impact oral cancers? Oral Oncol. 2020;104:104607. https://doi.org/10.1016/j.oraloncology.2020.104607.
20. Seeburg DP, Baer AH, Aygun N. Imaging of patients with head and neck cancer: from staging to surveillance. Oral Maxillofac Surg Clin North Am. 2018;30(4):421–33. https://doi.org/10.1016/j.coms.2018.06.004.
21. Mahajan A, Ahuja A, Sable N, Stambuk HE. Imaging in oral cancers: a comprehensive review. Oral Oncol. 2020;104:104658. https://doi.org/10.1016/j.oraloncology.2020.104658.
22. Bongers MN, Schabel C, Thomas C, et al. Comparison and combination of dual-energy- and iterative-based metal artefact reduction on hip prosthesis and dental implants. PLoS One. 2015;10(11):e0143584. https://doi.org/10.1371/journal.pone.0143584.
23. Huang SH, O'Sullivan B. Overview of the 8th edition TNM classification for head and neck cancer. Curr Treat Options in Oncol. 2017 Jul;18(7):40.
24. Thust SC, Yousry T. Imaging of skull base tumours. Rep Pract Oncol Radiother. 2016;21(4):304–18. https://doi.org/10.1016/j.rpor.2015.12.008.
25. Kuno H, Onaya H, Fujii S, Ojiri H, Otani K, Satake M. Primary staging of laryngeal and hypopharyngeal cancer: CT, MR imaging and dual-energy CT. Eur J Radiol. 2014 Jan;83(1):e23–35. https://doi.org/10.1016/j.ejrad.2013.10.022.
26. Frunza A, Slavescu D, Lascar I. Perineural invasion in head and neck cancers - a review. J Med Life. 2014;7(2):121–3.
27. Amit M, Eran A, Billan S, et al. Perineural spread in noncutaneous head and neck cancer: new insights into an old problem. J Neurol Surg B Skull Base. 2016;77(2):86–95. https://doi.org/10.1055/s-0036-1571834.
28. Yoo GH, Hocwald E, Korkmaz H, et al. Assessment of carotid artery invasion in patients with head and neck cancer. Laryngoscope. 2000;110(3 Pt 1):386–90. https://doi.org/10.1097/00005537-200003000-00010.
29. Chengazi HU, Bhatt AA. Pathology of the carotid space. Insights Imaging. 2019;10(1):21. https://doi.org/10.1186/s13244-019-0704-z.
30. Yousem DM, Gad K, Tufano RP. Resectability issues with head and neck cancer. AJNR Am J Neuroradiol. 2006;27(10):2024–36.
31. Sekine T, Barbosa FG, Delso G, Burger IA, Stolzmann P, Ter Voert EE, Huber GF, Kollias SS, von Schulthess GK, Veit-Haibach P, Huellner MW. Local resectability assessment of head and neck cancer: positron emission tomography/MRI versus positron emission tomography/CT. Head Neck. 2017 Aug;39(8):1550–8.
32. Tshering Vogel DW, Zbaeren P, Thoeny HC. Cancer of the oral cavity and oropharynx. Cancer Imaging. 2010;10(1):62–72. Published 2010 Mar 16. https://doi.org/10.1102/1470-7330.2010.0008.
33. Nae A, O'Leary G, Feeley L, Fives C, Fitzgerald B, Chiriac E, Sheahan P. Utility of CT and MRI in assessment of mandibular involvement in oral cavity cancer. World J Otorhinolaryngol Head Neck Surg. 2019;5(2):71–5. https://doi.org/10.1016/j.wjorl.2019.02.001.
34. Tamaki A, Miles BA, Lango M, Kowalski L, Zender CA. AHNS series: do you know your guidelines? Review of current knowledge on laryngeal cancer. Head Neck. 2018;40(1):170–81. https://doi.org/10.1002/hed.24862.

35. Shayah A, Wickstone L, Kershaw E, Agada F. The role of cross-sectional imaging in suspected nasopharyngeal carcinoma. Ann R Coll Surg Engl. 2019;101(5):325–7. https://doi.org/10.1308/rcsann.2019.0025.
36. Becker M, Burkhardt K, Dulguerov P, Allal A. Imaging of the larynx and hypopharynx. Eur J Radiol. 2008;66(3):460–79. https://doi.org/10.1016/j.ejrad.2008.03.027.
37. Dmytriw AA, El Beltagi A, Bartlett E, et al. CRISPS: a pictorial essay of an acronym to interpreting metastatic head and neck lymphadenopathy. Can Assoc Radiol J. 2014;65(3):232–41. https://doi.org/10.1016/j.carj.2013.07.004.
38. Pfister DG, Spencer S, Adelstein D, et al. Head and neck cancers, version 2.2020, NCCN clinical practice guidelines in oncology. J Natl Compr Cancer Netw. 2020;18(7):873–98. https://doi.org/10.6004/jnccn.2020.0031.
39. Dwivedi RC, Agrawal N, Dwivedi RC, Pathak KA, Kazı R. Evaluation, management and outcomes of head and neck cancer. In: Staffieri A, Sebastian P, Kapre M, Varghese BT, Kazı R, editors. Essentials of head and neck cancer. Delhi: Byword Books Private Limited; 2012. p. 19–33.
40. Merritt RM, Williams MF, James TH, Porubsky ES. Detection of cervical metastasis. A meta-analysis comparing computed tomography with physical examination. Arch Otolaryngol Head Neck Surg. 1997;123(2):149–52. https://doi.org/10.1001/archotol.1997.01900020027004.
41. Liao LJ, Lo WC, Hsu WL, Wang CT, Lai MS. Detection of cervical lymph node metastasis in head and neck cancer patients with clinically N0 neck-a meta-analysis comparing different imaging modalities. BMC Cancer. 2012;12:236. Published 2012 Jun 12. https://doi.org/10.1186/1471-2407-12-236.
42. Wu LM, Xu JR, Liu MJ, et al. Value of magnetic resonance imaging for nodal staging in patients with head and neck squamous cell carcinoma: a meta-analysis [published correction appears in Acad Radiol. 2012;19(6):674]. Acad Radiol. 2012;19(3):331–40. https://doi.org/10.1016/j.acra.2011.10.027.
43. Sun J, Li B, Li CJ, et al. Computed tomography versus magnetic resonance imaging for diagnosing cervical lymph node metastasis of head and neck cancer: a systematic review and meta-analysis. Onco Targets Ther. 2015;8:1291–313. https://doi.org/10.2147/OTT.S73924.
44. Lee KJ, Kirsch C, Sayre JW, Bhuta S, Abemayor E. Lymph node clustering in head and neck squamous cell cancer. Otolaryngol Head Neck Surg. 2008;139(2_Suppl):P39–40. https://doi.org/10.1016/j.otohns.2008.05.130.
45. Amin MB, Edge SB. AJCC cancer staging manual; 2017 (Print).
46. Lodder WL, Lange CA, Teertstra HJ, Pameijer FA, van den Brekel MW, Balm AJ. Value of MR and CT imaging for assessment of internal carotid artery encasement in head and neck squamous Cell carcinoma. Int J Surg Oncol. 2013;2013:968758. https://doi.org/10.1155/2013/968758.
47. Som PM. Detection of metastasis in cervical lymph nodes: CT and MR criteria and differential diagnosis. AJR Am J Roentgenol. 1992;158(5):961–9. https://doi.org/10.2214/ajr.158.5.1566697.
48. Ahuja AT, Ying M, Ho SY, et al. Ultrasound of malignant cervical lymph nodes. Cancer Imaging. 2008;8(1):48–56. https://doi.org/10.1102/1470-7330.2008.0006.
49. de Bondt RB, Nelemans PJ, Bakers F, et al. Morphological MRI criteria improve the detection of lymph node metastases in head and neck squamous cell carcinoma: multivariate logistic regression analysis of MRI features of cervical lymph nodes. Eur Radiol. 2009;19(3):626–33. https://doi.org/10.1007/s00330-008-1187-3.
50. Hoang JK, Vanka J, Ludwig BJ, Glastonbury CM. Evaluation of cervical lymph nodes in head and neck cancer with CT and MRI: tips, traps, and a systematic approach. AJR Am J Roentgenol. 2013;200(1):W17–25. https://doi.org/10.2214/AJR.12.8960.
51. Ying M, Bhatia KS, Lee YP, Yuen HY, Ahuja AT. Review of ultrasonography of malignant neck nodes: greyscale, Doppler, contrast enhancement and elastography. Cancer Imaging. 2014;13(4):658–69. https://doi.org/10.1102/1470-7330.2013.0056.
52. Pehlivan M, Gurbuz MK, Cingi C, Adapinar B, Değirmenci AN, Acikalin FM, Pinarbaşli MÖ, Colak E. Diagnostic role of ultrasound elastography on lymph node metastases in patients with head and neck cancer. Braz J Otorhinolaryngol. 2019;85(3):297–302. https://doi.org/10.1016/j.bjorl.2018.01.002.
53. Vandecaveye V, De Keyzer F, Vander Poorten V, et al. Head and neck squamous cell carcinoma: value of diffusion-weighted MR imaging for nodal staging. Radiology. 2009;251(1):134–46. https://doi.org/10.1148/radiol.2511080128.
54. Barchetti F, Pranno N, Giraldi G, et al. The role of 3 tesla diffusion-weighted imaging in the differential diagnosis of benign versus malignant cervical lymph nodes in patients with head and neck squamous cell carcinoma. Biomed Res Int. 2014;2014:532095. https://doi.org/10.1155/2014/532095.
55. Lim HK, Lee JH, Baek HJ, et al. Is diffusion-weighted MRI useful for differentiation of small non-necrotic cervical lymph nodes in patients with head and neck malignancies? Korean J Radiol. 2014;15(6):810–6. https://doi.org/10.3348/kjr.2014.15.6.810.
56. Mazzaferri EL, Kloos RT. Clinical review 128: current approaches to primary therapy for papillary and follicular thyroid cancer. J Clin Endocrinol Metab. 2001;86(4):1447–63. https://doi.org/10.1210/jcem.86.4.7407.
57. Kouvaraki MA, Shapiro SE, Fornage BD, et al. Role of preoperative ultrasonography in the surgical man-

agement of patients with thyroid cancer. Surgery. 2003;134(6):946–55. https://doi.org/10.1016/s0039-6060(03)00424-0.
58. Cooper DS, Doherty GM, et al. American Thyroid Association (ATA) Guidelines Taskforce on Thyroid Nodules and Differentiated Thyroid Cancer, Revised American Thyroid Association management guidelines for patients with thyroid nodules and differentiated thyroid cancer [published correction appears in Thyroid. 2010;20(8):942. Hauger, Bryan R [corrected to Haugen, Bryan R]] [published correction appears in Thyroid. 2010;20(6):674–5]. Thyroid. 2009;19(11):1167–214. https://doi.org/10.1089/thy.2009.0110.
59. Russ G, Leboulleux S, Leenhardt L, Hegedüs L. Thyroid incidentalomas: epidemiology, risk stratification with ultrasound and workup. Eur Thyroid J. 2014;3(3):154–63. https://doi.org/10.1159/000365289.
60. Burman KD, Wartofsky L. Thyroid nodules. N Engl J Med. 2016;374(13):1294–5. https://doi.org/10.1056/NEJMc1600493.
61. Koo BS, Choi EC, Park YH, Kim EH, Lim YC. Occult contralateral central lymph node metastases in papillary thyroid carcinoma with unilateral lymph node metastasis in the lateral neck. J Am Coll Surg. 2010;210(6):895–900. https://doi.org/10.1016/j.jamcollsurg.2010.01.037.
62. Zhao Q, Ming J, Liu C, et al. Multifocality and total tumor diameter predict central neck lymph node metastases in papillary thyroid microcarcinoma. Ann Surg Oncol. 2013;20(3):746–52. https://doi.org/10.1245/s10434-012-2654-2.
63. Na DG, Baek JH, Sung JY, et al. Thyroid imaging reporting and data system risk stratification of thyroid nodules: categorization based on solidity and echogenicity. Thyroid. 2016;26(4):562–72. https://doi.org/10.1089/thy.2015.0460.
64. Gharib H, Papini E, Garber JR, et al., American Association of Clinical Endocrinologists, American College of Endocrinology, Associazione Medici Endocrinologi. Medical guidelines for clinical practice for the diagnosis and management of thyroid nodules. 2016 update. Endocr Pract. 2016;22(5):622–39. https://doi.org/10.4158/EP161208.GL.
65. Tessler FN, Middleton WD, Grant EG, et al. ACR thyroid imaging, reporting and data system (TI-RADS): white paper of the ACR TI-RADS committee. J Am Coll Radiol. 2017;14(5):587–95. https://doi.org/10.1016/j.jacr.2017.01.046.
66. Grant EG, Tessler FN, Hoang JK, et al. Thyroid ultrasound reporting lexicon: white paper of the ACR thyroid imaging, reporting and data system (TIRADS) committee. J Am Coll Radiol. 2015;12(12 Pt A):1272–9. https://doi.org/10.1016/j.jacr.2015.07.011.
67. Russ G, Bonnema SJ, Erdogan MF, Durante C, Ngu R, Leenhardt L. European thyroid association guidelines for ultrasound malignancy risk stratification of thyroid nodules in adults: the EU-TIRADS. Eur Thyroid J. 2017;6(5):225–37. https://doi.org/10.1159/000478927.
68. Grani G, Lamartina L, Ascoli V, et al. Reducing the number of unnecessary thyroid biopsies while improving diagnostic accuracy: toward the "right" TIRADS. J Clin Endocrinol Metab. 2019;104(1):95–102. https://doi.org/10.1210/jc.2018-01674.
69. Grani G, Lamartina L, Cantisani V, Maranghi M, Lucia P, Durante C. Interobserver agreement of various thyroid imaging reporting and data systems. Endocr Connect. 2018;7(1):1–7. https://doi.org/10.1530/EC-17-0336.
70. Grani G, Lamartina L, Biffoni M, et al. Sonographically estimated risks of malignancy for thyroid nodules computed with five standard classification systems: changes over time and their relation to malignancy. Thyroid. 2018;28(9):1190–7. https://doi.org/10.1089/thy.2018.0178.
71. Ito Y, Higashiyama T, Takamura Y, et al. Risk factors for recurrence to the lymph node in papillary thyroid carcinoma patients without preoperatively detectable lateral node metastasis: validity of prophylactic modified radical neck dissection. World J Surg. 2007;31(11):2085–91. https://doi.org/10.1007/s00268-007-9224-y.
72. Langer JE, Mandel SJ. Sonographic imaging of cervical lymph nodes in patients with thyroid cancer. Neuroimaging Clin N Am. 2008;18(3):479, viii. https://doi.org/10.1016/j.nic.2008.03.007.
73. Hwang HS, Orloff LA. Efficacy of preoperative neck ultrasound in the detection of cervical lymph node metastasis from thyroid cancer. Laryngoscope. 2011;121(3):487–91. https://doi.org/10.1002/lary.21227.
74. Kim E, Park JS, Son KR, Kim JH, Jeon SJ, Na DG. Preoperative diagnosis of cervical metastatic lymph nodes in papillary thyroid carcinoma: comparison of ultrasound, computed tomography, and combined ultrasound with computed tomography. Thyroid. 2008;18(4):411–8. https://doi.org/10.1089/thy.2007.0269.
75. Leboulleux S, Girard E, Rose M, et al. Ultrasound criteria of malignancy for cervical lymph nodes in patients followed up for differentiated thyroid cancer. J Clin Endocrinol Metab. 2007;92(9):3590–4. https://doi.org/10.1210/jc.2007-0444.
76. Gimm O, Rath FW, Dralle H. Pattern of lymph node metastases in papillary thyroid carcinoma. Br J Surg. 1998;85(2):252–4. https://doi.org/10.1046/j.1365-2168.1998.00510.x.
77. Machens A, Hinze R, Thomusch O, Dralle H. Pattern of nodal metastasis for primary and reoperative thyroid cancer. World J Surg. 2002;26(1):22–8. https://doi.org/10.1007/s00268-001-0176-3.
78. Kuna SK, Bracic I, Tesic V, Kuna K, Herceg GH, Dodig D. Ultrasonographic differentiation of benign from malignant neck lymphadenopathy in thyroid

cancer. J Ultrasound Med. 2006;25(12):1531–40. https://doi.org/10.7863/jum.2006.25.12.1531.
79. Jiang ZZ, Huang YH, Shen HL, Liu XT. Clinical applications of superb microvascular imaging in the liver, breast, thyroid, skeletal muscle, and carotid plaques. J Ultrasound Med. 2019;38(11):2811–20. https://doi.org/10.1002/jum.15008.
80. Ahuja AT, Ying M, Ho SS, Metreweli C. Distribution of intranodal vessels in differentiating benign from metastatic neck nodes. Clin Radiol. 2001;56(3):197–201. https://doi.org/10.1053/crad.2000.0574.
81. Cibas ES, Ali SZ. The Bethesda system for reporting thyroid cytopathology. Thyroid. 2009;19(11):1159–65. https://doi.org/10.1089/thy.2009.0274.
82. Yang J, Schnadig V, Logrono R, Wasserman PG. Fine-needle aspiration of thyroid nodules: a study of 4703 patients with histologic and clinical correlations. Cancer. 2007;111(5):306–15. https://doi.org/10.1002/cncr.22955.
83. Roy R, Kouniavsky G, Venkat R, et al. The role of preoperative neck ultrasounds to assess lymph nodes in patients with suspicious or indeterminate thyroid nodules. J Surg Oncol. 2012;105(6):601–5. https://doi.org/10.1002/jso.22115.
84. Yeh MW, Bauer AJ, Bernet VA, et al. American Thyroid Association statement on preoperative imaging for thyroid cancer surgery. Thyroid. 2015;25(1):3–14. https://doi.org/10.1089/thy.2014.0096.
85. Hoang JK, Raduazo P, Yousem DM, Eastwood JD. What to do with incidental thyroid nodules on imaging? An approach for the radiologist. Semin Ultrasound CT MR. 2012;33(2):150–7. https://doi.org/10.1053/j.sult.2011.12.004.
86. Razek AA, Sadek AG, Kombar OR, Elmahdy TE, Nada N. Role of apparent diffusion coefficient values in differentiation between malignant and benign solitary thyroid nodules. AJNR Am J Neuroradiol. 2008;29(3):563–8. https://doi.org/10.3174/ajnr.A0849.
87. Van der Molen AJ, Thomsen HS, Morcos SK, Contrast Media Safety Committee, European Society of Urogenital Radiology (ESUR). Effect of iodinated contrast media on thyroid function in adults. Eur Radiol. 2004;14(5):902–7. https://doi.org/10.1007/s00330-004-2238-z.
88. Seo YL, Yoon DY, Lim KJ, et al. Locally advanced thyroid cancer: can CT help in prediction of extrathyroidal invasion to adjacent structures? AJR Am J Roentgenol. 2010;195(3):W240–4. https://doi.org/10.2214/AJR.09.3965.
89. Wang JC, Takashima S, Takayama F, et al. Tracheal invasion by thyroid carcinoma: prediction using MR imaging. AJR Am J Roentgenol. 2001;177(4):929–36. https://doi.org/10.2214/ajr.177.4.1770929.
90. Takashima S, Takayama F, Wang J, Kobayashi S, Kadoya M. Using MR imaging to predict invasion of the recurrent laryngeal nerve by thyroid carcinoma. AJR Am J Roentgenol. 2003;180(3):837–42. https://doi.org/10.2214/ajr.180.3.1800837.
91. Nam IC, Park JO, Joo YH, Cho KJ, Kim MS. Pattern and predictive factors of regional lymph node metastasis in papillary thyroid carcinoma: a prospective study. Head Neck. 2013;35(1):40–5. https://doi.org/10.1002/hed.22903.
92. Machens A, Holzhausen HJ, Dralle H. Skip metastases in thyroid cancer leaping the central lymph node compartment. Arch Surg. 2004;139(1):43–5. https://doi.org/10.1001/archsurg.139.1.43.
93. Kaplan SL, Mandel SJ, Muller R, Baloch ZW, Thaler ER, Loevner LA. The role of MR imaging in detecting nodal disease in thyroidectomy patients with rising thyroglobulin levels. AJNR Am J Neuroradiol. 2009;30(3):608–12. https://doi.org/10.3174/ajnr.A1405.
94. Schlüter B, Bohuslavizki KH, Beyer W, Plotkin M, Buchert R, Clausen M. Impact of FDG PET on patients with differentiated thyroid cancer who present with elevated thyroglobulin and negative 131I scan. J Nucl Med. 2001;42(1):71–6.
95. Som PM, Lawson W, Genden EM. The posttreatment neck: clinical and imaging considerations. In: Som PM, Curtin HD, editors. Head and neck imaging. 5th ed. St Louis, MO: Mosby; 2011. p. 2771–822.
96. Manikantan K, Khode S, Dwivedi RC, et al. Making sense of post-treatment surveillance in head and neck cancer: when and what of follow-up. Cancer Treat Rev. 2009;35(8):744–53. https://doi.org/10.1016/j.ctrv.2009.08.007.
97. Subramaniam RM, Truong M, Peller P, Sakai O, Mercier G. Fluorodeoxyglucose-positron-emission tomography imaging of head and neck squa- mous cell cancer. AJNR Am J Neuroradiol. 2010;31(4):598–604. https://doi.org/10.3174/ajnr.A1760.
98. de Bree R, van der Putten L, Brouwer J, Castelijns JA, Hoekstra OS, Leemans CR. Detection of locoregional recurrent head and neck cancer after (chemo) radiotherapy using modern imaging. Oral Oncol. 2009;45(4–5):386–93. https://doi.org/10.1016/j.oraloncology.2008.10.015.
99. Yao M, Smith RB, Graham MM, et al. The role of FDG PET in management of neck metastasis from head-and-neck cancer after definitive radiation treatment. Int J Radiat Oncol Biol Phys. 2005;63(4):991–9. https://doi.org/10.1016/j.ijrobp.2005.03.066.
100. Vandecaveye V, De Keyzer F, Nuyts S, et al. Detection of head and neck squamous cell carcinoma with diffusion weighted MRI after (chemo) radiotherapy: correlation between radiologic and histopathologic findings. Int J Radiat Oncol Biol Phys. 2007;67(4):960–71. https://doi.org/10.1016/j.ijrobp.2006.09.020.
101. Vandecaveye V, De Keyzer F, Dirix P, Lambrecht M, Nuyts S, Hermans R. Applications of diffusion-weighted magnetic resonance imaging in head and

neck squamous cell carcinoma. Neuroradiology. 2010;52(9):773–84. https://doi.org/10.1007/s00234-010-0743-0.

102. Genden EM, Rinaldo A, Suárez C, Wei WI, Bradley PJ, Ferlito A. Complications of free flap transfers for head and neck reconstruction following cancer resection. Oral Oncol. 2004;40(10):979–84. https://doi.org/10.1016/j.oraloncology.2004.01.012.
103. Lell M, Baum U, Greess H, et al. Head and neck tumors: imaging recurrent tumor and post-therapeutic changes with CT and MRI. Eur J Radiol. 2000;33(3):239–47. https://doi.org/10.1016/s0720-048x(99)00120-5.
104. Makimoto Y, Yamamoto S, Takano H, et al. Lymphadenopathy in the mesenteric pedicle of the free jejunal flap: reactive lymphadenopathy, not metastatic. J Comput Assist Tomogr. 2006;30(1):65–7. https://doi.org/10.1097/01.rct.0000177606.90817.cb.
105. Chong VF. Post treatment imaging in head and neck tumours. Cancer Imaging. 2005;5(1):8–10. Published 2005 Apr 6. https://doi.org/10.1102/1470-7330.2005.0003.
106. Mukherji SK, Wolf GT. Evaluation of head and neck squamous cell carcinoma after treatment. AJNR Am J Neuroradiol. 2003;24(9):1743–6.
107. Hermans R. Posttreatment imaging in head and neck cancer. Eur J Radiol. 2008;66(3):501–11. https://doi.org/10.1016/j.ejrad.2008.01.0210.1186/1758-3284-3-14.